AD 261 566

AFSWC-TN-61-14

SWC
TN
61-14

HEADQUARTERS

AIR FORCE SPECIAL WEAPONS CENTER

AIR FORCE SYSTEMS COMMAND

KIRTLAND AIR FORCE BASE, NEW MEXICO

75 900

DESIGN AND ANALYSIS OF FOUNDATIONS FOR PROTECTIVE STRUCTURES

Second Interim Technical Report

by

K. E. McKee

Armour Research Foundation
of
Illinois Institute of Technology
Chicago, Illinois

May 1961

61-4-3
NOX

HEADQUARTERS
AIR FORCE SPECIAL WEAPONS CENTER
Air Force Systems Command
Kirtland Air Force Base, New Mexico

Major General Charles M. McCorkle
Commander

Colonel Carey L. O'Bryan, Jr.
Deputy Commander

Colonel Leonard A. Eddy
Director Research Directorate

AFSWC-TN-61-14

DESIGN AND ANALYSIS OF FOUNDATIONS

FOR PROTECTIVE STRUCTURES

Second Interim Technical Report

by

K. E. McKee

Armour Research Foundation

of

Illinois Institute of Technology

Technology Center

Chicago 16, Illinois

May 1961

Research Directorate
AIR FORCE SPECIAL WEAPONS CENTER
Air Force Systems Command
Kirtland Air Force Base, New Mexico

Approved:

Leonard A. Eddy

LEONARD A. EDDY
Colonel USAF
Director, Research Directorate

Project No. 1080

Task No. 10803

Contract No. AF 29(601)-2561

ABSTRACT

The behavior of footings subjected to time-dependent forces is the subject of continuing research. The approach to this research is twofold: Theoretical and experimental. This interim report is concerned with the experimental results and comparisons to the theoretical approaches.

Two- and three-dimensional footings on Ottawa sand were loaded dynamically using the loading apparatus and instrumentation developed for this program. The two-dimensional experiments permitted observation of the behavior on loose and dense sand subjected to vertical, inclined, and eccentric dynamic loads. The three-dimensional experiments provided force-time and displacement-time records of the behavior on dense sand of vertically loaded footings.

These experiments demonstrate that the theories developed previously on this program are not satisfactory. They also indicate the direction to be taken in future theoretical research.

In an attempt to consider additional soils, California sand and clays were studied. A series of static loadings of three-dimensional footings were conducted on California sand. Static and dynamic loads were applied to two-dimensional footings on clay. It was established that the static loads were truly static by experiments conducted at low rates of loading.

PUBLICATION REVIEW

This report has been reviewed and is approved.

for Felix H. Jones, Col.
WILLIAM N. [illegible]ETTORE
Colonel USAF
Deputy Chief of Staff/Operations

PREFACE

This is the second interim technical report on Contract No. AF29(601)-2561, Project 1080, "Design and Analysis of Foundations for Protective Structures". The objective of this research program is to investigate the problems associated with the design and analysis of foundations for protective structures subjected to dynamic loads from nuclear blast. The current project, initiated at Armour Research Foundation in February 1960, is, to a large extent, a continuation of research done on an earlier contract AF29(601)1161 of the same title.

The first interim report, dated September 1960, covered the technical work up to that date. This publication reports the research conducted since that time. In this report, the primary technical results are collected into appendices, which will subsequently be incorporated into the final report.

Personnel contributing to the work described in this report include C.J. Costantino, A. Humphreys, K.E. McKee, R.D. Rowe, S. Shenkman, and E. Vey. The author thanks Mr. C. Wiehle and Mr. H. Mason of Air Force Special Weapons Center for their criticisms and suggestions which have materially aided this project.

TABLE OF CONTENTS

LIST OF TABLES

LIST OF ILLUSTRATIONS

APPENDICES

LIST OF ILLUSTRATIONS, cont.

Chapter 1

INTRODUCTION

A. General

Protective construction has in the past few years become a problem of substantial interest to the structural engineer. The foundations for such structures presented particularly difficult problems since there was little information available. This publication reports on a continuing research program conducted at Armour Research Foundation dealing with "the design and analysis of foundations for protective structures subjected to dynamic loads from nuclear blast". Specifically, this report covers the research done subsequent to that reported in the Interim Technical Report dated September 1960.

The reader is assumed to be familiar with the results of previous ARF research in this technical area. The results of the original study, conducted under Contract No. AF29(601)-1161, are summarized in AFSWC TR-59-56 (8)*. More details regarding certain aspects of the research under that contract are found in the three phase reports: Phase Report I, "Recommendations for Full-Scale Tests", issued October 15, 1958; Phase Report II, "Bibliography on Foundations Subjected to Dynamic Loads", issued December 31, 1958; and Phase Report III, "Interim Technical Report", issued January 31, 1959. Research under the present contract (AF29(601)-2561) up to September 1960 has been previously reported (12).

For all practical purposes, ARF research into the behavior of foundations subjected to dynamic loads has represented a continuing effort. There has been no repetition of previous research; although this report has been written to make it readable without supplementary references. Practical

---

* Numbers in parentheses cite references listed as Appendix H.

detailed technical presentations are confined to the appendices of this report with the main body limited to a general presentation of results, discussions, comparisons and conclusions.

B. Technical Objective

"To investigate the problems associated with the design and analysis of foundations for protective structures which are subjected to dynamic loads from nuclear blasts" is the general objective as stated in the contract. This definition is, naturally, quite broad; therefore, the technical direction of the program must dependon more special technical objectives mutually acceptable to ARF and the Air Force. Under the current contract, consideration is limited to spread footings as contrasted with more general "foundations". During the original project it was postulated that, at least from a qualitative point-of-view, foundations could be divided into spread footings and pile foundations. The assumption was that the behavior of all footings could be explained in terms of these two, idealized, footing types or some combination of them.

With regard to the spread footing, the primary research goal has been to achieve an understanding of the behavior of footings on arbitrary soil to an arbitrary time-dependent force. The method of approach has been a combination of experimental and theoretical research. The theoretical research has attempted to develop analytical models which would satisfactorily explain the footing behavior. The experimental research has been directed toward proving or disproving the suitability of the analytical model. In addition, experiments have been designed to obtain qualitative information to aid in modifying existing analytical approaches or in developing new approaches.

C. Discussion of the Problem

Literature on the behavior of footings under dynamic loads is quite extensive. Almost without exception however, this literature relates the behavior of footings subjected to periodic sinusoidal forcing functions. For this class of problem the soil obviously must not fail; to a large extent, the case reduces to the determination of an effective mass of soil for inclusion as part of a mass-spring system. Although the problem of footing vibration is one of fundamental importance, it is of relatively little significance for dynamically loaded footings used in protective structures. Footings for protective structures are subjected to forces having an arbitrary time-history which may be a single force pulse as contrasted with repetitious small force pulses.

Various analytical approaches have been suggested in connection with footings for protective structures. These approaches are, in general, based on modified static approaches and are justified only by engineering intuition. The author knows of a single previous program which included experimental studies of the behavior of footings subjected to dynamic loads. In 1954, Massachusetts Institute of Technology conducted limited static and dynamic footing tests (6) (7). Currently three other agencies are testing footings subjected to dynamic loads: Naval Civil Engineering Laboratory, Port Hueneme, California; University of Illinois, Urbana, Illinois; and Waterways Experiment Station, Vicksburg, Mississippi. For information covering these programs, the reader is referred directly to these agencies.

The present research project has provided quantitative data relating to the behavior of small footings subjected to dynamic loads. Vertical loads applied to footings on limited soil types provided the bulk of these experiments. Sufficient data have been collected to allow comparisons to the analytical approaches which have been developed. The results of these comparisons are discussed later in this report.

D. Report Organization

The main body of this report is primarily descriptive in nature. Chapter 2 reports on the results of the research which is presented in greater detail in the appendices. Chapter 3 considers the theoretical approach which has been developed to predict the behavior of footings subjected to dynamic loads. Chapter 4 is devoted to interpretations of the experimental results and comparisons of these to analytical predictions. Chapter 5 presents the general conclusions and indicates the direction for future research.

The appendices deal with specific aspects of the project. The first six appendices deal with various phases of the experimental program, while Appendix G contains a nomenclature descriptive of the notations used throughout this report. Appendix H lists the references.

Chapter 2

EXPERIMENTAL RESEARCH

A. General

This chapter reports the experimental research conducted during the period covered by this report. Details of this research are presented in the six appendices to this report. In compiling this chapter, liberal references are made to these appendices. In discussing the experimental research, the limitations and questionable features are considered along with the successes and advantages.

B. Dynamic Loading Apparatus and Instrumentation

Appendix A, by Mr. S. Shenkman, describes the apparatus developed at ARF for applying dynamic forces. This pneumatic-hydraulic loading device was described in less complete fashion in the earlier report on this project (14). Basically, this apparatus applies a time-dependent force to the footing; instrumentation is provided to measure the applied force-time history and resultant displacement-time history of the footing. The ARF dynamic loader proved to be quite satisfactory. Substantial ranges of force-time history could be achieved by altering the controls used in the setup. Some parameters, such as the rise-time, were not varied on this program since only the rapid rise time was desired, although the equipment has provisions built into it for this purpose. Moreover, since only general requirements of force-time histories were placed on the equipment, which could be readily monitored by suitable instrumentation, it was possible to construct the dynamic loader with a striking simplicity conducive to reliable operation.

C. Two-Dimensional Dynamically Loaded Footings

The ARF dynamic loader was used to apply concentric vertical, eccentric vertical, and inclined forces to two-dimensional footings on both loose and dense Ottawa sand. Preliminary work on these experiments was described in the previous report on this contract (13). By using the glass-sided container, it was possible to obtain "before" and "after" photographs and high speed movies of soil failures. The experiments conducted, techniques employed, and typical results obtained are presented as Appendix B.

The high-speed motion pictures provide a tool for improved qualitative understanding of the footing behavior. The films themselves, as well as sequenced photographs printed from them, permit observation of the complete motion of the footing. Displacement-time data, of course, can be measured directly from the film. The peak and the general trend of the applied force are also available although quantitative results are of questionable value because of the interaction of the footings with the sides of the container. For this reason, the two-dimensional experiments provide primarily qualitative data.

D. Three-Dimensional Dynamically Loaded Footings

Quantitative experimental data were collected for small three-dimensional footings. These experiments were conducted in the 4-ft x 4-ft x 3-ft box used during the original program. Dynamic loads were applied by dropping weights and by using ARF pneumatic-hydraulic loader. Details of these experiments are contained in Appendix C. Because of recording system response limitations, the force-time history associated with the dropped weight could not be satisfactorily recorded. Alternate recording systems could have been incorporated into the experimental setup but such modifications were not considered justified for the current program. Consequently the dropped-weight experiments were terminated.

In general, the results of the dynamically loaded footing experiments were satisfactory. Prior to the experiments reported in Appendix C, a series of experiments was conducted to learn to control the apparatus and to get some indication of the magnitude of the responses which could be anticipated. The results of this preliminary work have no quantitative meaning, and hence are not reported.

E. Statically Loaded Footings on California Sand

The Naval Civil Engineering Laboratory, Port Hueneme, California, has initiated an experimental program using their Blast Simulator to apply dynamic loads to footings. The soil they are using is a local sand; herein referred to simply as California sand. The initial information required for this comparison regards the behavior of small footings loaded statically when the soil is California sand.

Suitable quantities of California sand were shipped from the West Coast. The sand box (4-ft x 4-ft x 3-ft) was filled with this sand and a limited experimental study was conducted of footings loaded statically. The results of this study are reported in detail in Appendix D. Essentially, the problems were the same as those observed for Ottawa sand. The total range of values for the angle of internal friction, ϕ, was 42.5° to 48°, with an average of approximately 46°. While this range of variation might be tolerable, small changes in ϕ involve large changes in bearing capacities, hence the bearing capacities show a wide range of values.

F. Effect of Loading Rate for Footings Placed on Ottawa Sand

Studies were initiated to determine how rapidly a load may be applied and still be considered as being static. Particularly, the question was whether loads applied by using hydraulic jacks could be considered static. The results indicated that the behavior of a footing loaded by means of a manually controlled hydraulic jack was comparable to that of the footing subjected to a much lower rate of load application. (The downward speed of the top of the proving ring was kept at 0.00053 in. per minute). These experiments did shed some light on the behavior of soil below footings when shear surfaces have formed. Details of these experiments are reported in Appendix E.

G. Footings on Cohesive Soils

The experimental research on the initial phases of this program considered the behavior of footings on dense Ottawa sand. Subsequent studies consider other cohesionless materials: loose Ottawa sand and the California sand discussed earlier. Obviously, one can not limit consideration of soils to cohesionless materials. For this reason, experimental studies were initiated under the current project to consider cohesive materials. The results of this research are reported in Appendix F.

Static and dynamic loads were applied to two-dimensional footings on cohesive soil in the glass-sided container. The primary purpose of this series of experiments was to obtain qualitative information relating to the behavior of footings on cohesive materials. In the process of conducting these experiments the sides of the glass container had to be reinforced to withstand the loads being transferred; the controls required to avoid segregation of the layers also had to be investigated. Altogether, the experimental results were encouraging since they indicated that such an approach was feasible.

Chapter 3

ANALYTICAL RESEARCH

A. Introduction

The previous chapter, supplemented by the appendices, reports the experimental studies conducted in the soil laboratory since the last report. During this period little theoretical research was performed. Laboratory work, however, was specifically oriented to provide data establishing the validity, or lack thereof, of the theoretical approaches developed during the course of this project. In this chapter the theory is summarized with special attention to the assumptions made and the resulting solution. The following chapter considers the comparison of experimental and analytical results.

B. Static Bearing Capacities

The literature provides many analyses for footing failures caused by shear failure in the soil below the footing. (Note that settlements caused by compressibility of the soil due to long duration load applications are of little interest here, since the loads of interest have durations of the order of seconds.) A number of theoretical approaches considered during this project are suitable for predicting the bearing capacities of footings subjected to static loads. The theory of plasticity, as discussed in the previous report (12) includes general methods of approach for such problems. For this project, the methods used for static loading are the less general, but simpler ones, normally used in soil mechanics. In the final report (8) on the original project, two one-sided failure and one two-sided failure solutions were discussed. The one-sided failure modes discussed were Andersen's (1) analysis and a modification of Krey's (4) analysis. For the two-sided or symmetrical failure patterns, Terzaghi's (17)(18) formula was used.

These three approaches have been found to give similar (within 10% of each other) values for the bearing capacity. Over the range of parameters of interest, Andersen's formula gives a load capacity which is essentially that given by Terzaghi's formula.(17), and Hasson (4) demonstrated that his formulation of Krey's method gives capacities similar to those given by Terzaghi's formula. It was also demonstrated experimentally, in connection with this research, that the bearing capacity appears to be essentially independent of the type of failure, i.e., one-sided or symmetrical.

For static bearing-capacity analyses performed in connection with this research project, Terzaghi's formula was normally accepted. The approximate formula developed by Terzaghi for infinitely long footings with rough bases is:

$$\frac{P_s}{A} = c\,N_c + \gamma\,D\,N_q + \frac{1}{2}\gamma\,B\,N_\gamma, \qquad \text{(Eq. 1)}$$

where A = footing area (ft^2)
B = footing width (ft),
c = cohesion (psf),
D = depth of burial (ft),
P_s = static bearing capacity (lb),
γ = density of soil (pcf),
ϕ = angle of internal friction of the soil (deg).

The quantities N_c, N_q, and N_γ are dimensionless bearing-capacity factors, depending only on the angle of internal friction, ϕ. The value of each of these factors can be plotted as a function of ϕ - such plots are given by Terzaghi (17) and Terzaghi and Peck (18). For square or circular footings, the approximate formula is modified by empirical coefficients.

Comparisons between this approximate formula and the experimental results have been generally satisfactory. Actually, because the density of the sand in the three-dimensional experiments was higher than had been obtained in the laboratory, the formula was used in reverse to obtain the angle of internal friction for the Ottawa and California sands. The results obtained in this way were consistent and represented a reasonable extrapolation of the values for the angle of internal friction consistent with values obtained by more normal soil mechanics procedures for these soils at lesser densities.

C. Behavior of Footings Subjected to Dynamic Loads

This section summarizes the analytical models which have been considered. Sufficient detail will be presented here to make the discussions in the next chapter understandable. Nonessential details and derivations are omitted.

The behavior of footings subjected to dynamic loads was treated in the original program (8) by what might be termed an "engineering approach". This approach was based on an extension to time-dependent loads of Andersen's (1) work relating to one-sided failure of the soil below the footing. Major assumptions introduced by this approach were:

i. The failure surface under dynamic loads will be the same as that determined for a similar static force considering the initial value of the overpressure to be applied as a static overburden.

ii. The resistance offered to movement is rigid plastic in form, i.e., settlement and soil compressibility are not considered.

iii. The maximum plastic resistance equals the static resistance determined analytically, assuming the failure surfaces considered are the same as in item i above.

iv. The behavior of the soil is governed by the parameters γ, ϕ, and c where ϕ and c may themselves be functions of many parameters relating to the soil and to the conditions of loading.

By considering the motion of the failure mass of soil, a differential equation was established for the dynamic behavior. Solutions of this equation allow prediction of the displacement and the investigation of inertia effects.

The dynamic equation was developed using the shear surface location (r) and static load capacity (P_s) determined by the static analysis to define the failure mass of soil. We emphasize that the determination of the static data should be based on the best estimate for the soil properties, i.e., the properties should be selected to incorporate the influence of the variables involved. (This would include effects such as the rate of load application, etc.) The static data, r and P_s, were tabulated in Appendix B of the report on the original project (8).

The equation governing dynamic behavior is given by:

$$I\ddot{\theta} + R(\theta) = M(t) \qquad \text{(Eq. 2)}$$

where

θ = rotation of soil mass,

$\ddot{\theta}$ = $d^2\theta/dt^2$ = acceleration,

I = rotational inertia,

$R(\theta)$ = resistance as a function of θ,

$M(t)$ = time-dependent moments.

If rotation about the center of the failure circle is considered, the terms in equations 2 can be written as:

$$I = \frac{\gamma}{g\left(1 - \frac{B}{2r}\right)} \left[0.64397\, r^3 + \frac{D}{3}(D^2 + r^2) + 0.78540\, r \left(\frac{4r}{3\pi} - D\right)^2 \right], \qquad \text{(Eq. 3)}$$

$$R(\theta) = \frac{\gamma\theta}{\left(r - \frac{B}{2}\right)} \left\{ 0.106\pi \left[r^3 + (r + D)^3 \tan\psi \right] - \frac{D\,(r - B)^2}{2} \tan\lambda \right\} \qquad \text{(Eq. 4)}$$

$$M(t) = P(t) - P_s + \frac{0.106\,\gamma\pi}{\left(r - \frac{B}{2}\right)} \left[r^3 - (r + D)^3 \right] + \frac{\gamma D\,(r - B)^2}{2\left(r - \frac{B}{2}\right)}, \qquad \text{(Eq. 5)}$$

where

ψ = $\tan^{-1}\left[\lambda - \frac{D}{0.424\,(r + D)}\right]$,

g = gravitational constant

B = width of footing,

r = dimension defining location of failure surfaces,

D = depth of burial of footing,

θ = rotation of soil mass about point C,

$P(t)$ = time-dependent forces applied to footing,

P_s = static capacity of footing,

$\lambda = \tan^{-1} \frac{D}{r - B}$,

γ = unit weight of soil.

Applications of the theory of plasticity to predict the behavior of footings subjected to dynamic loads was also initiated as part of this project. Hodge (5) considered the problem for a material which exhibited an ideal rigid-plastic behavior. An alternate mathematical approach was published by Spencer (16). The plasticity approach is limited in several respects. The idealization of the material properties raises serious doubts regarding the applicability of the solutions to real soils. In addition, the complexity of the solutions are such that, at least for the present, these approaches can not be expected to yield readily useable results. In spite of current limitations, the plasticity approaches may offer the only practical means of obtaining a complete understanding of the phenomena involved. For our present purposes, however, the plasticity approaches are of little direct usefulness and will essentially be neglected.

Chapter 4

COMPARISON OF EXPERIMENTAL RESULTS WITH THE THEORETICAL APPROACHES

A. Introduction

In the previous chapter the theoretical approaches were discussed in general terms. The modified soil mechanics approaches are based on certain common assumptions related to rigid body behavior of masses of soil. The resulting dynamic approaches therefore all assume the same form. For this reason, it is possible to establish, in general, the suitability of this type approach within certain limits. For this purpose the one-sided failure mode and the resulting dynamic equations will be used.

The experimental results used for this comparison are the three-dimensional footings on Ottawa sand. The experimental procedures, the results, etc. are presented as Appendix C. The measured force-time and displacement-time records which were obtained are of interest here.

Figure 1 presents the curves obtained for three static experiments using 4 in. x 4 in. footings and are reproduced from the report on the original project (8). Figure 2 shows an average curve for this size footing based on the three experiments plotted in figure 1.

B. Initial Approaches

As indicated in the previous chapter, the theoretical approaches are based on the assumption that the resistance to dynamic loads is similar to that for static loads. The initial attempts to interpret the data were therefore, based on this assumption. By using the measured force-time curve from dynamic experiments and resistance curves based on the static information, it is relatively simple to calculate the displacement-time history which would be predicted by the analysis. This analytical result could then be compared directly with the measured displacement-time history. These considerations dictated the selection of the displacement as one of the quantities to be measured.

The first attempt to analyze the data obtained from the dynamically loaded three-dimensional footing was based on this approach. There is

PRECEDING PAGE BLANK

little merit in reciting the type of modifications considered to make the static resistance-displacement curve suitable. It is sufficient to say that there was no reasonable modification which resulted in a calculated displacement-time curve even resembling those recorded in the laboratory.

At this stage it became obvious that the resistance displacement for dynamic loads bore little resemblance to that for static loads. The assumption that these curves could be related to each other in some relatively simple way was shown to be in error. The analytical approach was revised and the data analyzed in a different fashion as is discussed in the following section.

C. Analysis of Data

The analytical approach adopted used the measured force-time and displacement-time records to determine the associated resistance-displacement relationship. As an intermediate step this procedure required determination of the acceleration-time history from the displacement-time records. Because of the sensitive nature of this determination, the analysis was viewed with considerable trepidation. Normal good practice avoids any procedure based on finding the second derivatives of experimental curves. Unfortunately, by the time the necessity for this procedure was established, it was too late to permit modification of the experimental procedure to incorporate measurements of the acceleration directly.

Consider a linearized equation of motion of the form

$$m\ddot{x} + R(x) = P(t) \qquad \text{(Eq. 6)}$$

where

m = equivalent mass,
x = vertical displacement,
$\ddot{x}$ = d^2x/dt^2 = vertical acceleration,
$R(x)$ = resistance as a function of vertical displacement,
$P(t)$ = applied vertical force as a function of time.

Note that this equation assumes a constant mass, a resistance which is dependent only on the displacement, and a force which is a function only of time. From the measured results the experiments provide F(t) directly and x as a function of time. Assuming that the mass, m, can be determined, equation 6 can be solved for R(x) using the acceleration determined from the x(t) data.

$$R(x) = F(t) - m\ddot{x}$$

This equation shows that at each instant the resistance, R, depends on the applied force, the mass, and the acceleration.

In the first attempt to apply this approach, four experiments, P27, P28, P29 and P30, were considered in detail. These records were selected since they were similar in nature and had all produced substantial displacements. The records of these four experiments were analyzed utilizing the accelerations computed from the displacement curves. Figure 3 shows points obtained from these analyses. The fact that the points on the R(x) curves for these four experiments are so well grouped was encouraging - a single curve can reasonably be drawn through the points. On the other hand, the variations of the points from a single experiment are indicative of inconsistencies introduced by determination of the acceleration. When alternate time intervals were used for determination of the acceleration the variations for a single experiment were as significant in magnitude, but showed no consistence with earlier results.

This procedure was subsequently carried out for eighteen experiments for which both the displacement and force data were satisfactory. Table 1 indicates the experiments considered. Table 2 shows an example (for Ex. No. P32) of calculations made. In this example, 5-msec time intervals were selected and values for displacement and force were read from the records at that interval. The mass, m, used was 0.0223 lb sec^2/in. based on the mass of the footing added to the soil in a half cylinder having radius and lengths equal to the footing dimensions. This relatively arbitrary determination of the mass was investigated by considering possible variations -- for all practical purposes, however, the inertial term is negligible over the range of possible values.

Figures 3 through 7 show the resistance-displacement curves computed in this fashion. The average static resistance-displacement (Fig. 2) is redrawn on each of these figures. The arrangement of the experiments on each of the five figures (3 - 7) merely attempts to collect those having approximately the same values of the resistance. Observe that there is little resemblance between the static and dynamic curves and, more significantly, between the curves computed based on the dynamic experiments. This contrasts with the uniformity demonstrated by the four results plotted on figure 3.

While much could be written regarding these calculated resistance-displacement-curves and their meaning, it is sufficient to say that they demonstrate the inappropriateness of using the static resistance, directly or with any simple modifications. This means that the assumptions on which the dynamic solutions have been based are not satisfactory. The type of dynamic analysis attempted, therefore, cannot be expected to provide a solution.

The development of a more suitable approach was not attempted during this program. Certain observations from the dynamic experiments, however, indicate the direction such a development must take. From the displacement records, both velocity and acceleration appear to start at zero. In terms of the previous dynamic analysis, this implies that the computed initial resistance is approximately equal to the initially applied force. Such behavior is certainly not to be expected from a rigid mass subjected to external forces as postulated for equation 3. This behavior is of the type observed for a compressible material. The general direction of the theoretical work will, therefore, consider the combination of stress wave propagation and shear failure in the soil.

Chapter 5

SUMMARY

The general approach from the inception of the project has made use of a double attack: theory and experimentation. The theoretical studies have been used as the basis for planning the experimental planning. Conversely, the experimental studies have served to assess the validity of the theoretical approaches and, in addition, provided a qualitative basis on which new theories could be developed.

Most of the research reported herein is associated with the experimental studies. The theoretical research completed earlier in the program was used as the basis for planning these experiments. The experimental results have been analyzed and compared with available theories. Detailed writeups are included covering the experimental procedure, results and evaluations.

The studies to date provide much information regarding small footing behavior. The research relating to behavior under static loads verifies, in general, classical shear surface approaches. One sided and symmetrical failure surfaces were observed and the bearing capacities have been correlated with those calculated from standard, soil mechanics equations. In the original program (8), dynamic loads were limited to dropped weights. This technique provided qualitative information and limited quantitative data for the footings tested. From these experiments, differences were observed in the mode of behavior of similar footings subjected to static and dynamic loads. To obtain further information, a more general type of dynamic loading was required. The equipment developed to provide these loads, along with the data which have been obtained, are considered fully in this report.

The experiments demonstrate that the analytical approach suggested for predictions of behavior of dynamically loaded footings is not satisfactory.

The principal problem to which continuing effort on this program must be directed, therefore, is the development of a realistic theoretical formula- tion of the behavior of footings under dynamic loads. We feel that sufficient experimental data are now available to permit such an undertaking without fear that an unsuitable model will again be used.

Table 1

EXPERIMENTS USED FOR ANALYSIS

Experiment No.	Peak Force (lb)	Figure with R(x) (Fig. No.)
P7	299	6
P8	137	5
P10	397	6
P11	476	7
P25	546	4
P27	159	3
P28	148	3
P29	123	3
P30	168	3
P31	371	7
P32	112	5
P38	366	7
P39	334	6
P40	303	6
P41	272	6
P42	270	6
P43	272	6
P44	332	6

Table 2

CALCULATIONS FOR EXPERIMENT NO. P32

Time (msec)	Force, F (lb)	Displ., x (in)	$\dot{x}$ (in./msec)	$\ddot{x}$ (in./msec^2)	$\ddot{x}$ (in./sec^2)	$m\ddot{x}$ (lb)	$R = F - m\ddot{x}$
0	0	0					
			0.00232				
5	72.58	0.0116		-0.000116	-116	-2.587	75.17
			0.00174				
10	101	0.0203		+0.000120	+120	+2.676	98.32
			0.00234				
15	83.80	0.0320		+0.000228	+228	+5.084	78.72
			0.00348				
20	98.76	0.0494		-0.000348	-348	-7.760	106.52
			0.00174				
25	86.04	0.0581		+0.000468	+468	+10.436	75.60
			0.00408				
30	87.54	0.0785		-0.000236	-236	-5.263	92.80
			0.00290				
35	94.27	0.0930		-0.000116	-116	-2.587	96.86
			0.00232				
40	82.30	0.1046		+0.000004	+ 4	0.089	82.21
			0.00234				
45	84.55	0.1163		-0.000004	- 4	-0.089	84.64
			0.00232				
50	87.55	0.1279		-0.000348	-348	-7.760	95.31
			0.00058				
55	74.82	0.1308		+0.000232	+232	+5.174	69.65
			0.00174				
60	80.06	0.1395		+0.000004	+ 4	0.089	79.97
			0.00176				
65	84.55	0.1483		-0.000352	-352	-7.850	92.40
			0				
70	74.82	0.1483		0	0	0	74.82
			0				
75	56.86	0.1483		-0.000352	-352	-7.850	64.71
			-0.00176				
80	11.22	0.1395		-0.002088	-2088	-46.562	57.78
			-0.01220				
85	0	0.0785					

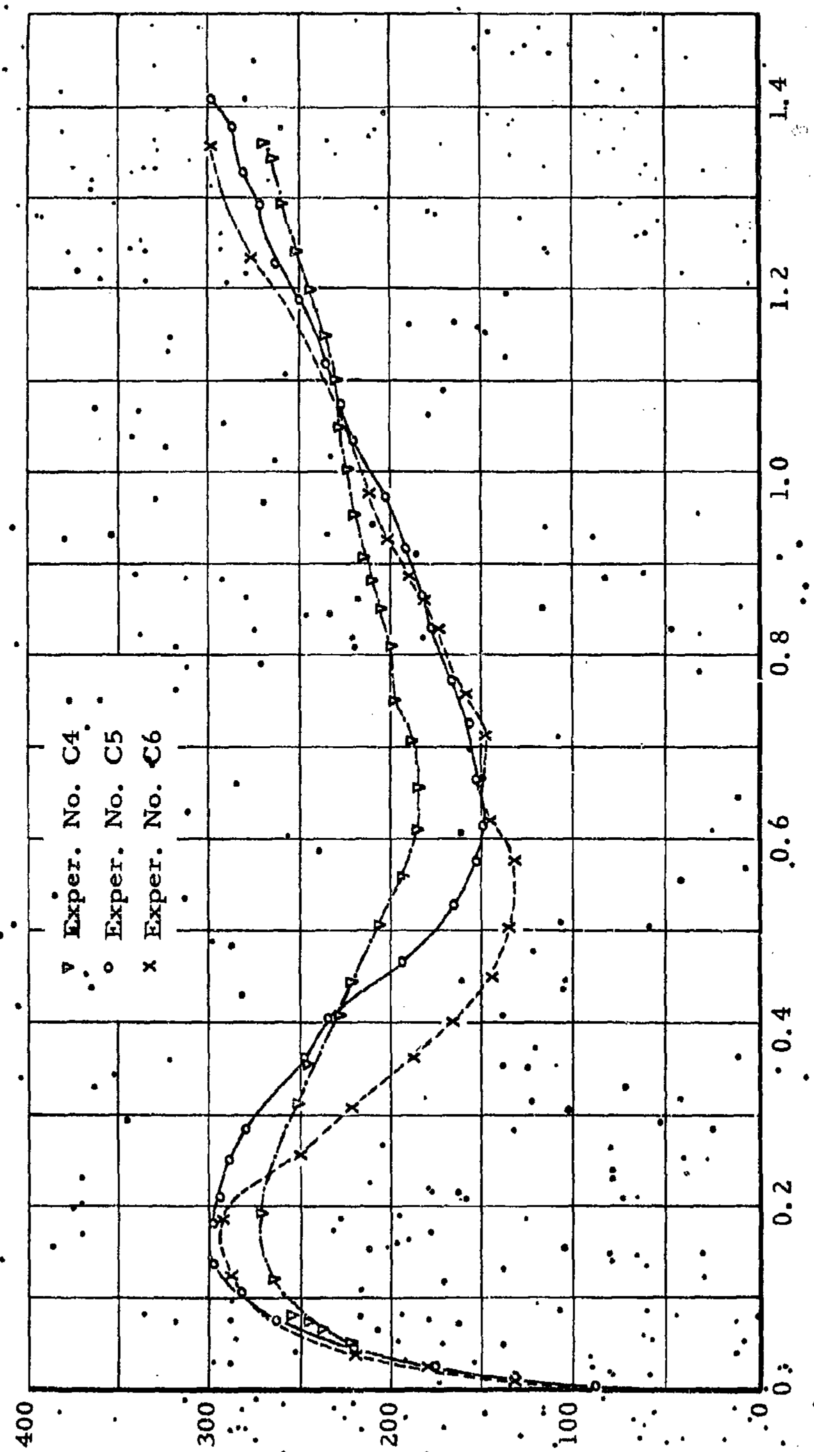

Fig. 1 STATIC LOAD-DISPLACEMENT MEASUREMENTS FOR 4-IN. SQUARE FOOTINGS

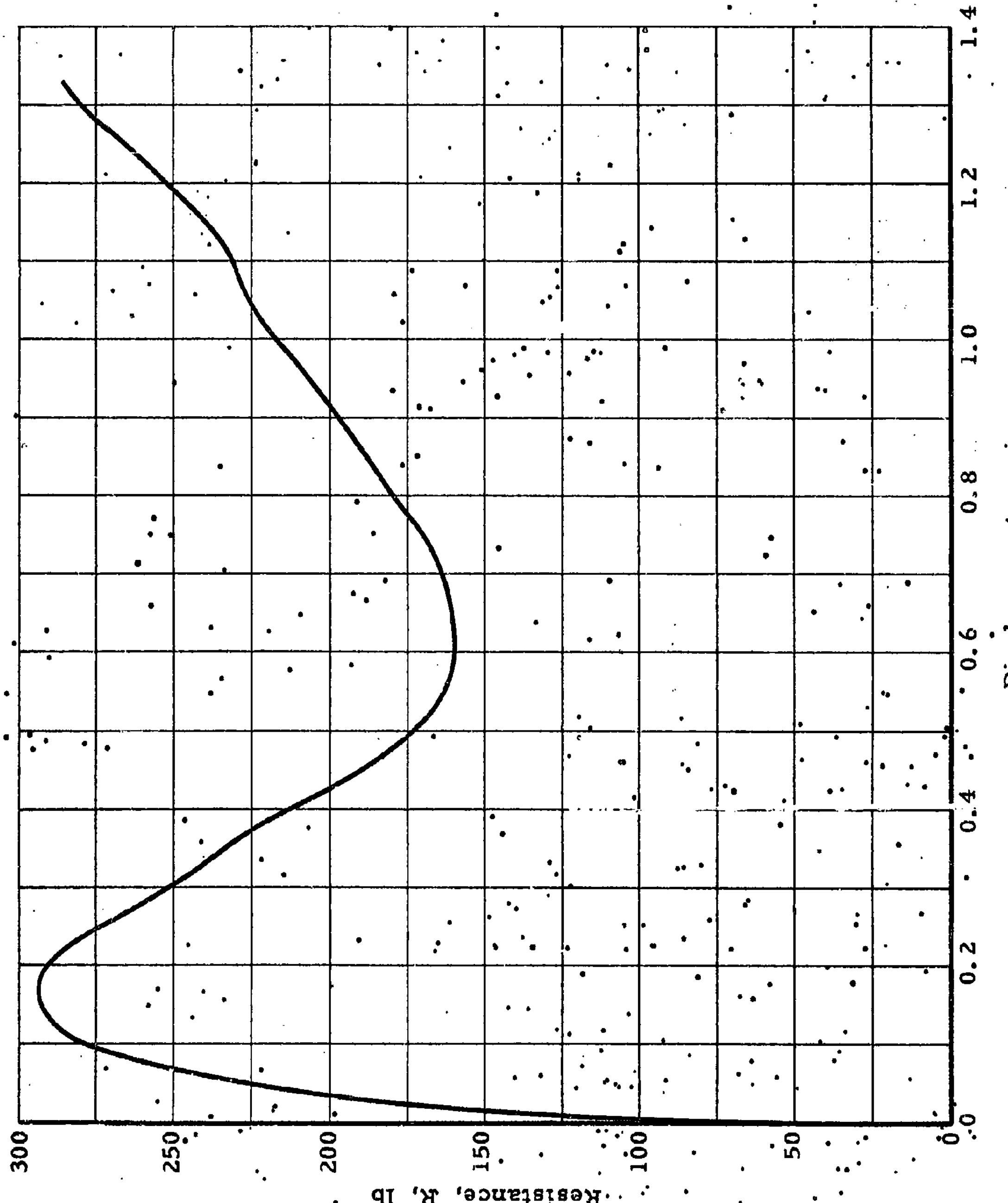

Fig. 2 AVERAGE STATIC RESISTANCE-DISPLACEMENT CURVE FOR 4-IN. SQUARE FOOTING

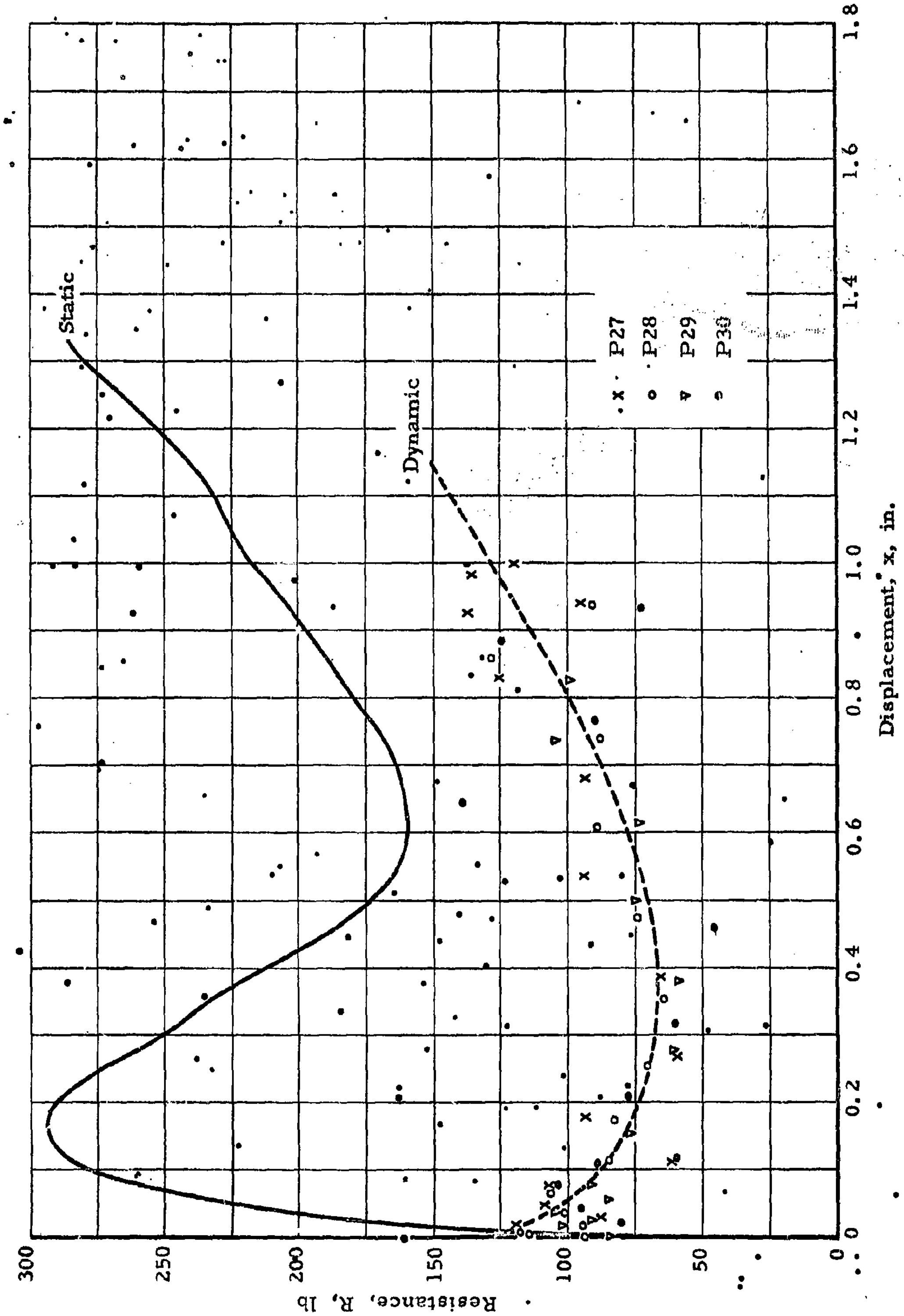

Fig. 3 RESISTANCES FOR EXPERIMENTS NO. P27, P28, P29 and P30

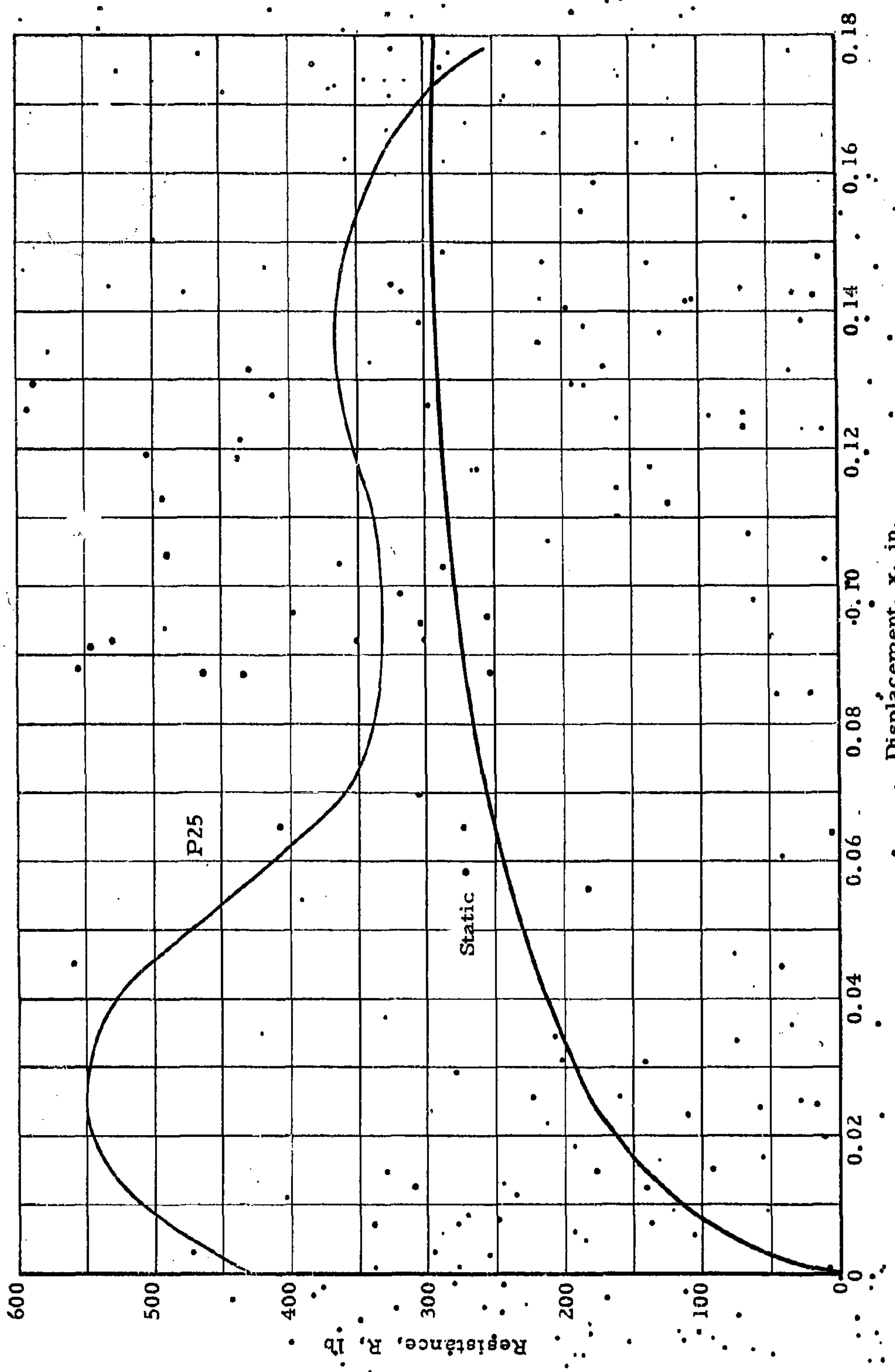

Fig. 4 RESISTANCE FOR EXPERIMENT NO. P25

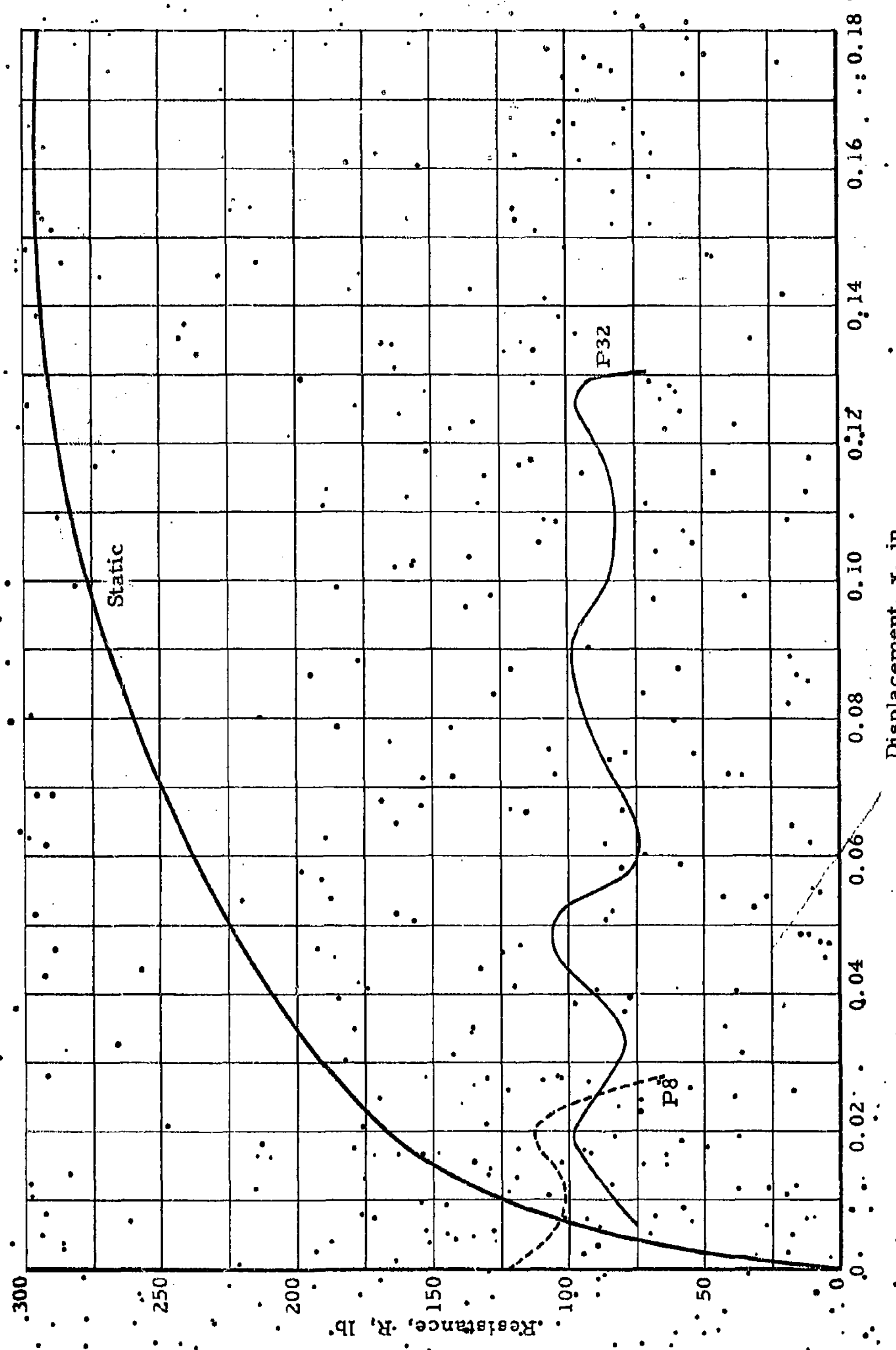

Fig. 5 RESISTANCE FOR EXPERIMENTS NO. P8 AND P32

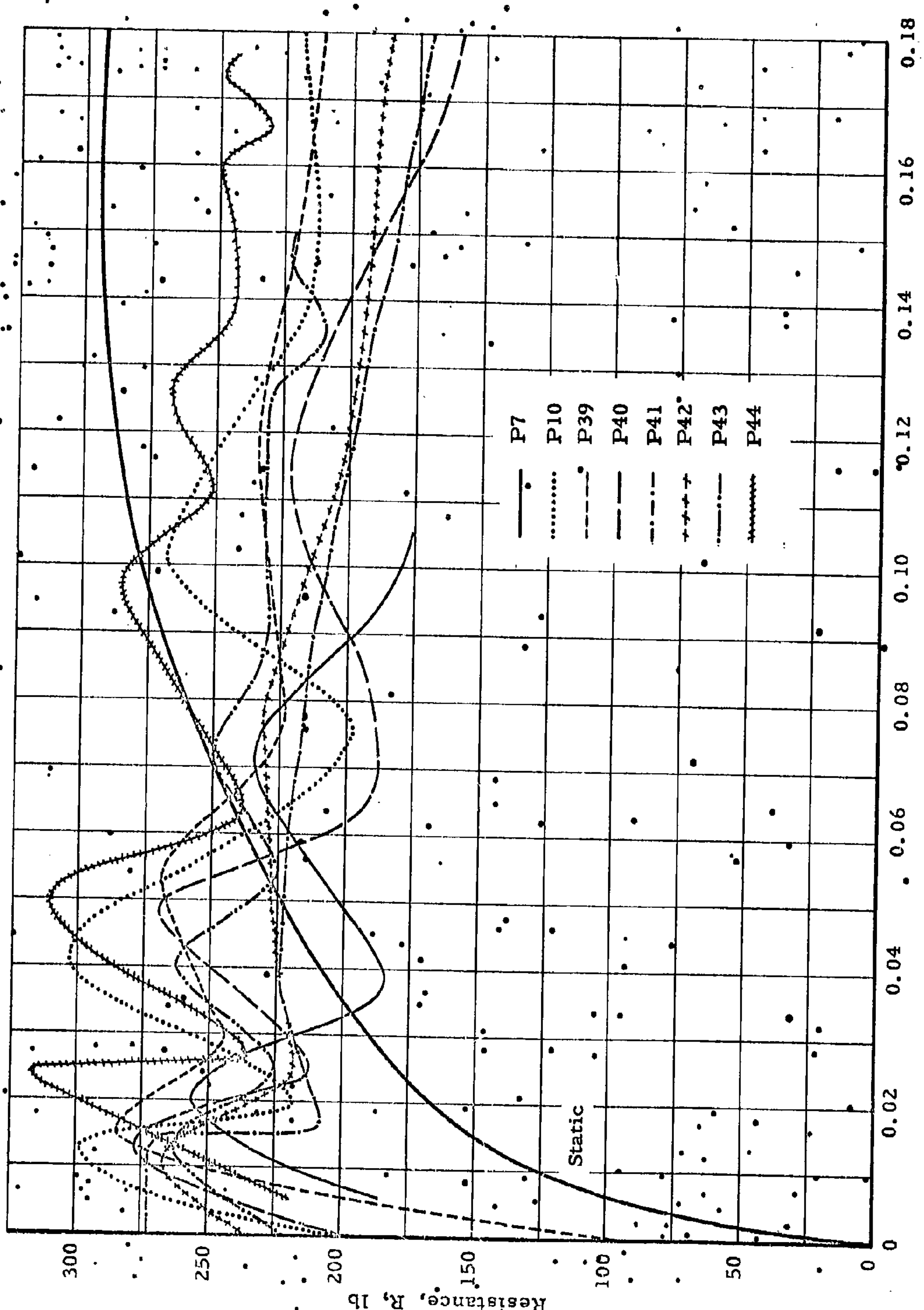

Fig. 6 RESISTANCES FOR EXPERIMENTS NO. P7, P10, P39, P40, P41, P42, P43 AND P44

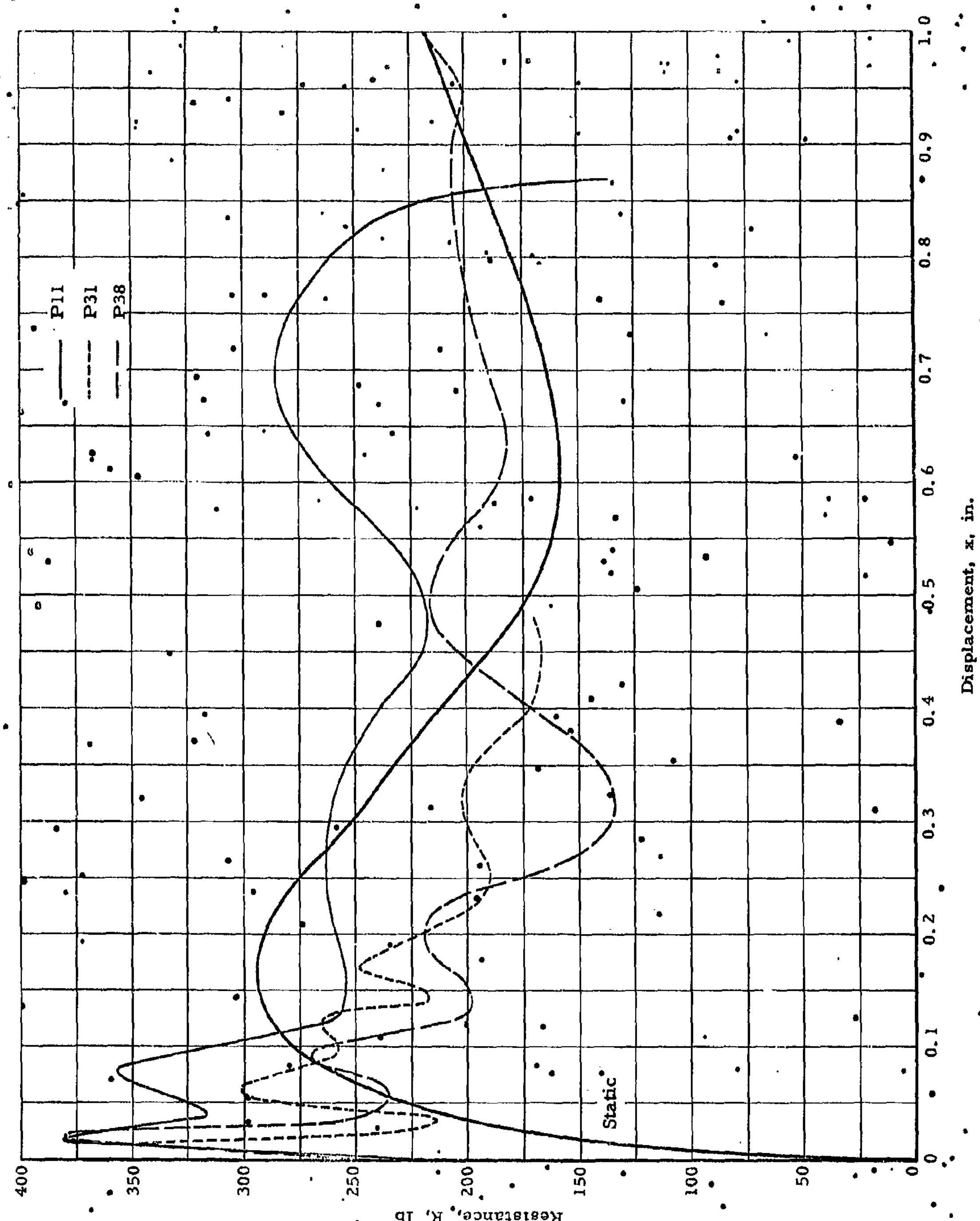

Fig. 7 RESISTANCES FOR EXPERIMENTS NO. P11, P31, AND P38

APPENDIX A

DYNAMIC LOADING APPARATUS AND INSTRUMENTATION

by S. Shenkman

APPENDIX A

DYNAMIC LOADING APPARATUS AND INSTRUMENTATION

by S. Shenkman

As part of the project it was necessary to design an apparatus suitable for applying dynamic loads to a small footing, as well as to select the appropriate instrumentation. The design of an apparatus capable of applying a load with specified time history presents a very difficult problem. However, if one is satisfied with a load which possesses only general characteristics, the task is simplified. For example, if one's interests lie in a type of load characterized by a very fast rise time (less than one millisecond) and a correspondingly fast decay time, a dropped weight may solve the experimental problem.

For this project it was decided that a load having a rapid rise time with a gradual decay time would be most suitable. This general form would be associated with blast loading from either a nuclear or high explosive detonation -- actually the transmission characteristic of the structure supported by an actual footing would produce a much more complex loading form. The general blast loading form was selected nevertheless since it is relatively simple and may have some relationship to the correct loading.

To produce this type of loading, a high pressure source was used with a quick opening valve, which permitted air to travel through an air cylinder actuating a piston. Results obtained by this method showed a moderately fast rise time (on the order of ten milliseconds) but a decay time time that was undesirably short.

A simple modification of this equipment, incorporating a hydraulic system rather than the air, yielded results which are quite satisfactory in both rise time and duration of loading. The dynamic loading apparatus finally developed applies dynamic loads characterized by a rise time on the order of two to five milliseconds; a slow decay, determined by the length of time the solenoid is actuated; and a sudden decay to zero force (approximately five milliseconds) after the hydraulic valve is closed.

The apparatus as sketched in figure A-1 consists of a nitrogen bottle, capable of delivering 2400 psi; an air pressure regulator; an air accumulator; a hydraulic accumulator; a solenoid operated hydraulic valve; and a hydraulic cylinder. The over-all apparatus is shown in figure A-2 and a detailed photograph of the hydraulic system in figure A-3.

Operation of the dynamic loading device is relatively simple. With the hydraulic valve closed, pressure is released from the nitrogen bottle into the air accumulator and the lower portion of the hydraulic accumulator. In this way a pre-determined pressure is built up in the fluid behind the hydraulic valve. When the valve is opened a dynamic load is applied to the piston.

A Barksdale, a.c. solenoid, 3-way, hydraulic valve is used as a flow control. The valve, in a normally closed position, provides a return of oil to the reservoir without opening needle valve A (Fig. A-1). Upon completion of a test, the oil transferred to the hydraulic cylinder was returned to the accumulator by opening needle valves A (to supplement the oil flow through the solenoid valve) and C and restoring the piston rod to its pre-loaded position.

Instrumentation for dynamic experiments on three-dimensional footings consisted of a Lockheed Electronics Model WR7S high sensitivity force washer and a Linear Variable Differential Transformer (henceforth referred to as an LVDT). The force washer, custom-built by Lockheed to required specifications, has a linear range of 0 to 1000 pounds. Load sleeves, provided with the washer, connect to the footing beneath the washer and to a steel ball above the washer. The ball acts as a roller between the hydraulic cylinder piston rod and the force washer.

The displacement of the footing was recorded by the LVDT, which measures the movement of the piston rod relative to the cylinder -- the assumption being that this measurement represents the displacement of the center of the footing. As shown in figure A-2, it was connected to a strip of steel cantilevered off the cylinder piston rod.

Dynamic recording was accomplished on a Consolidated Electro-Dynamics Corporation recorder. The CEC oscillograph is a strip chart recorder with a one-millisecond response time. As shown in figure A-4, the recording system was run independently of the solenoid valve. The CEC recorder was permitted to reach full running speed (25 in. per sec) before energizing the solenoid valve.

Instrumentation for dynamic experiments in the glass box (11) was limited to high speed movie photography. A 16mm Wallensak Fastax camera, running at 2000 frames per second, was used for this purpose. Film speed of the camera was determined by timing lights which exposed the edges of the film. A two-second delay was used to enable the camera to reach full running speed before energizing the hydraulic valve.

A time delay, incorporated in the system, permitted the solenoid valve to remain open for varying periods of time. In this manner, the valve is controlled electrically for a range of 13 to 70 milliseconds or manually for any other period of time. More accurate determinations of the length of time the valve remained open may be made by observing the records. Figures A-5 and A-6 are examples of force-time and displacement-time histories obtained for controlled openings of 70 and 13 milliseconds, respectively. Figure A-5 shows the period of time from initial rise of the force to the start of the sudden decay to be 77 milliseconds. Since the opening was set for 70 milliseconds, a close approximation for the duration of the loading may be made from the original input. A more peaked-type load (Fig. A-6) was applied when the solenoid remained open for 13 milliseconds.

The apparatus may be further modified to eliminate the sharp decay in force. This is accomplished either by capping the oil return in the solenoid or placing a needle valve in the line, thereby controlling the rate at which oil will return once the solenoid is closed.

Dynamic loading is not limited to vertical concentric applications. Experiments have been conducted using the pneumatic-hydraulic loader to produce eccentric and inclined loads. An example of an inclined loading setup on the glass box is shown in figure A-7. In general the ARF pneumatic-hydraulic dynamic loading apparatus has proven extremely flexible as to the types of loading outputs which are available.

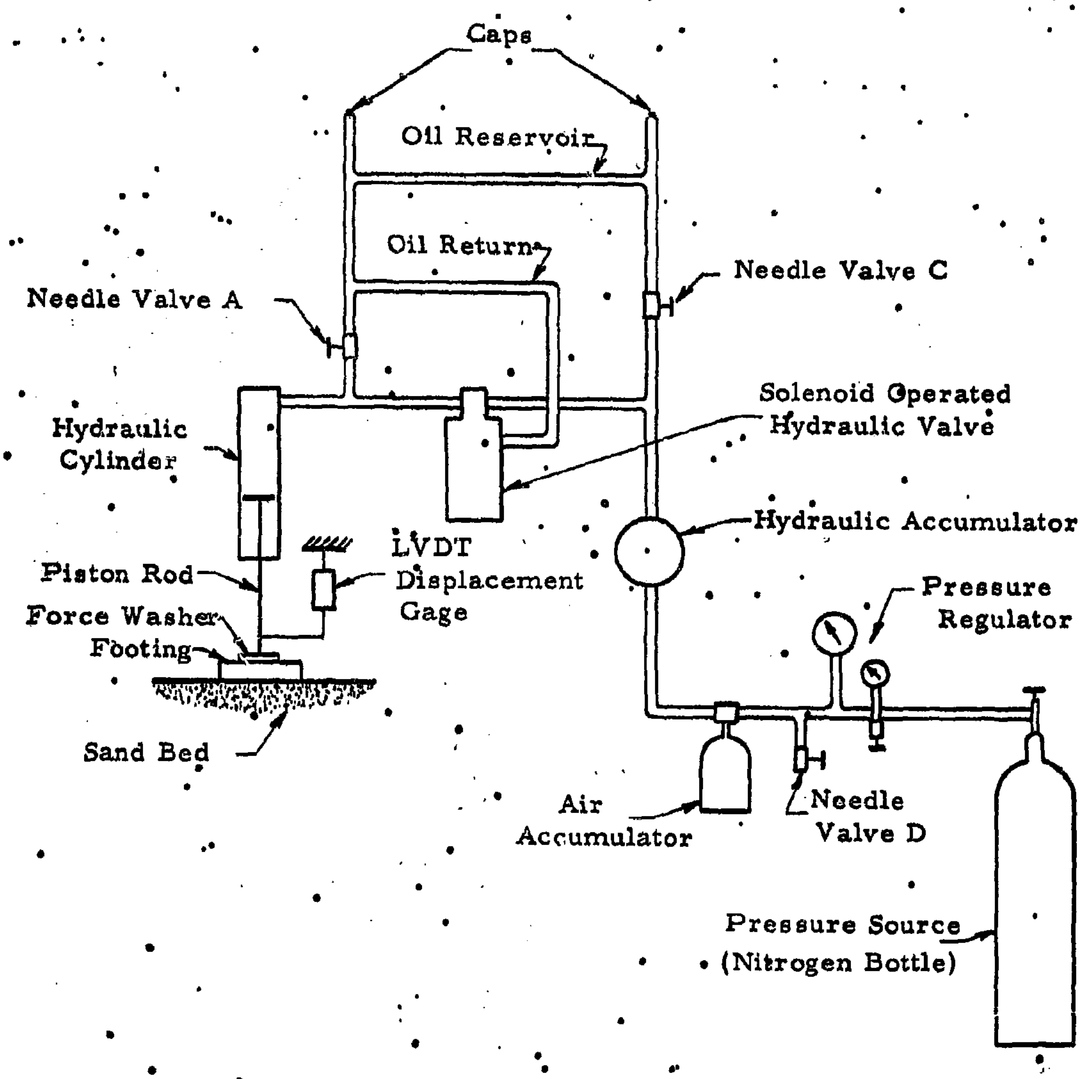

Fig. A-1 SKETCH OF DYNAMIC APPARATUS

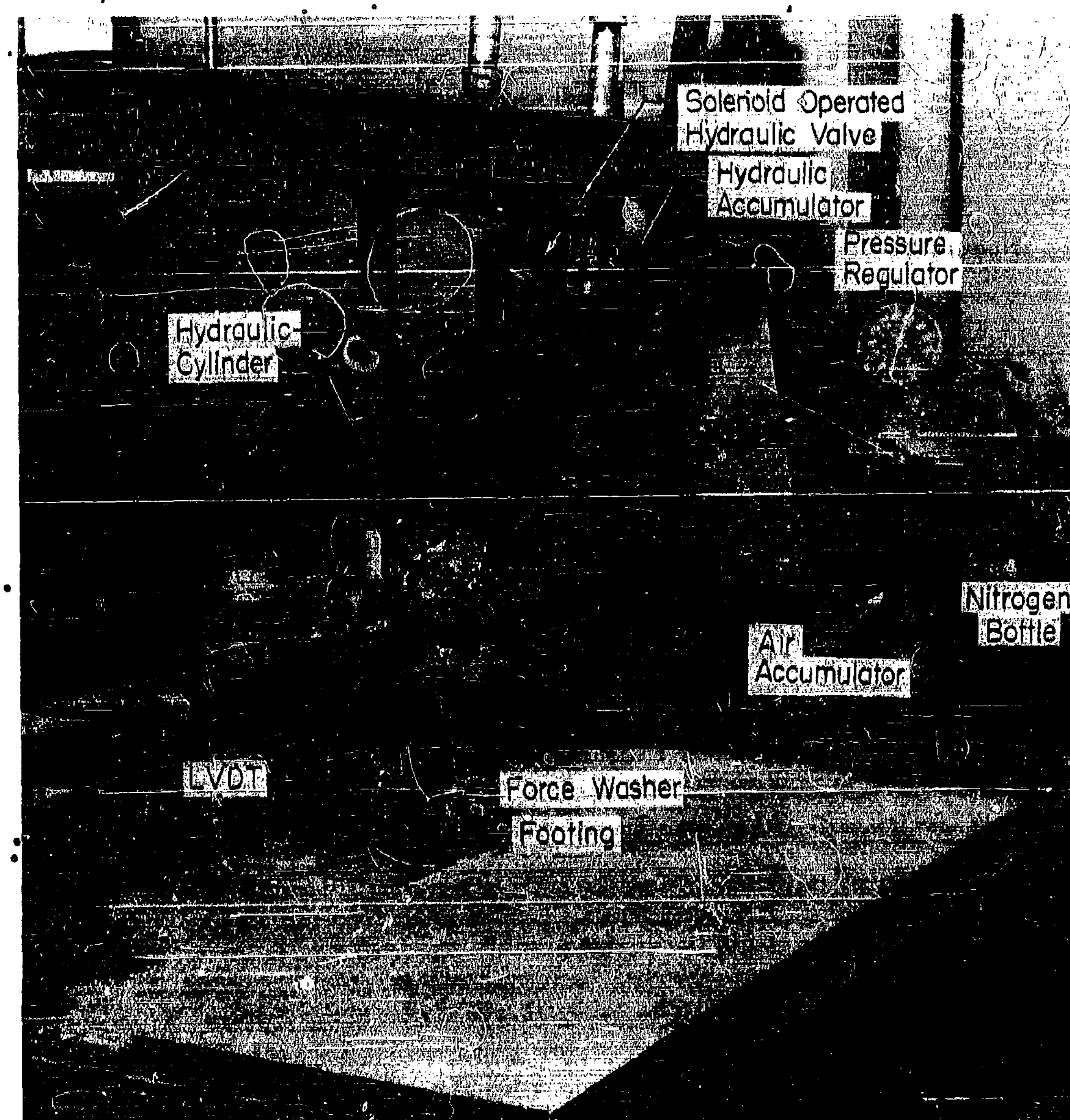

Fig. A-2 PHOTOGRAPH OF DYNAMIC APPARATUS

Fig. A-3 HYDRAULIC SYSTEM

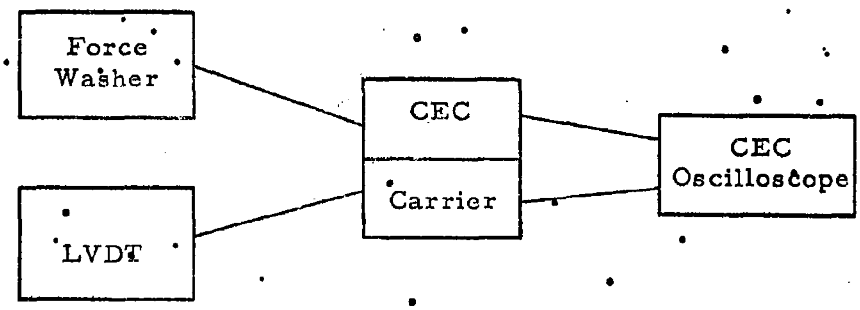

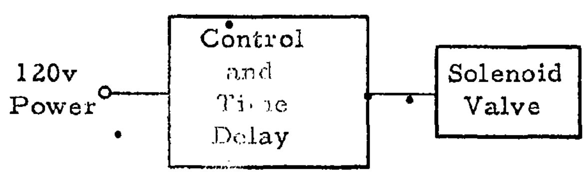

Fig. A-4 SCHEMATIC DIAGRAM OF CONTROL AND RECORDING EQUIPMENT

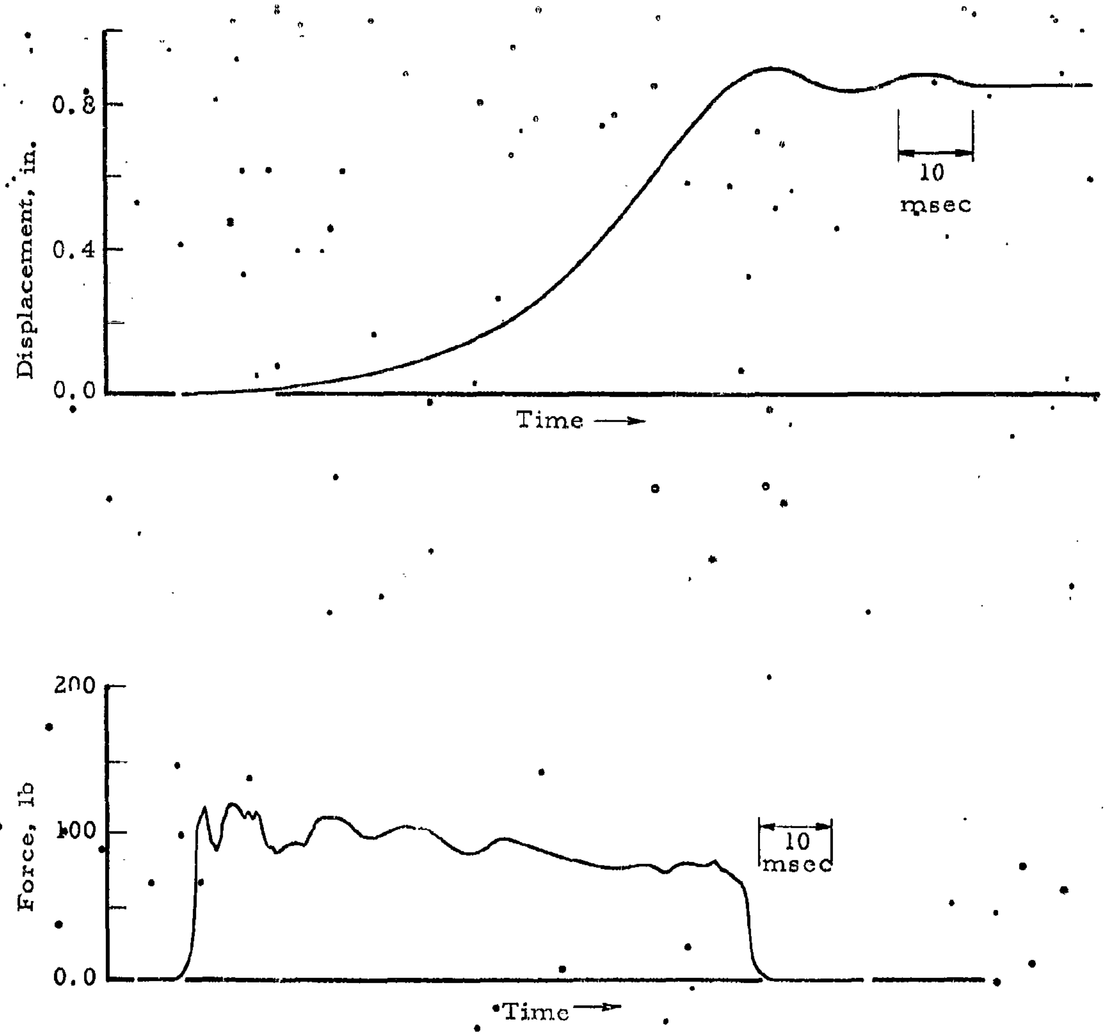

Fig. A-5 FORCES AND DISPLACEMENTS FOR 70 MSEC VALVE OPENING

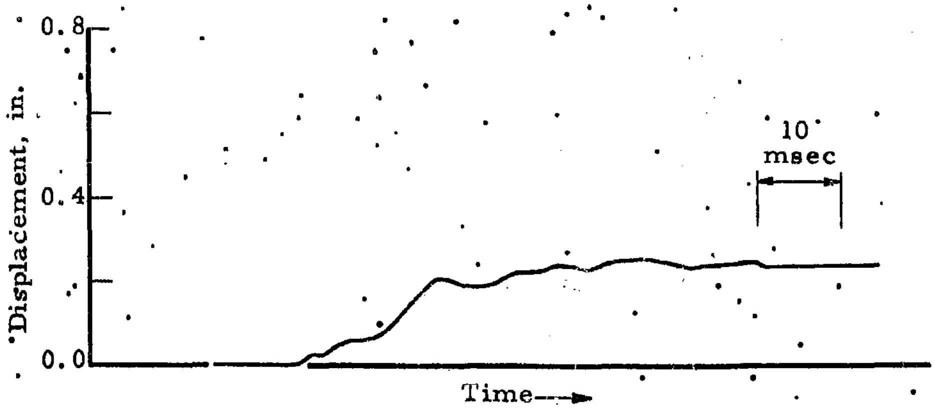

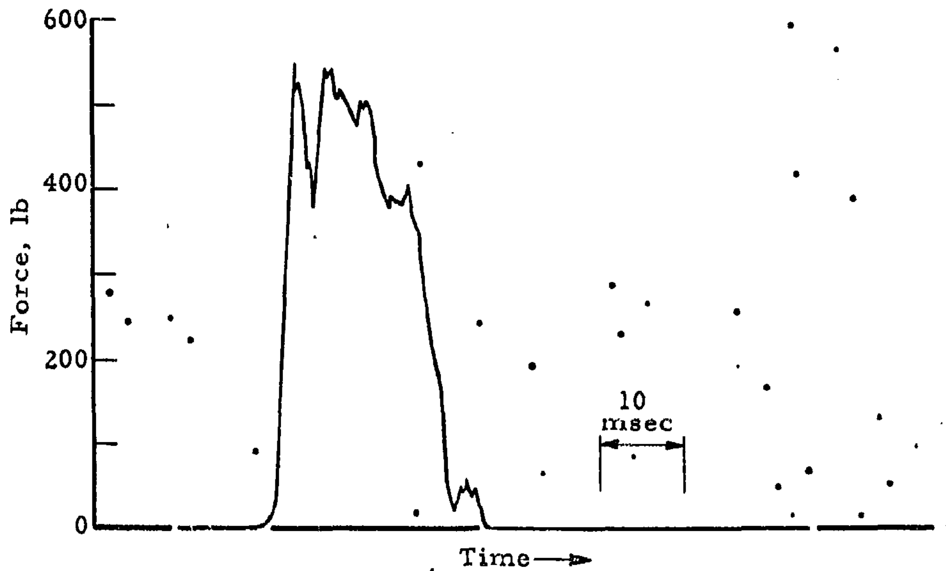

Fig. A-6 FORCES AND DISPLACEMENTS FOR 13 MSEC VALVE OPENING

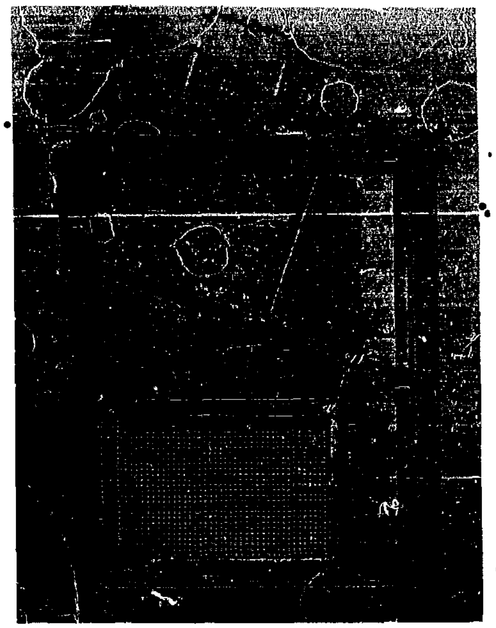

Fig. A-7 INCLINED LOADING SETUP ON GLASS BOX

APPENDIX B

TWO-DIMENSIONAL DYNAMIC EXPERIMENTS ON OTTAWA SAND

APPENDIX B

TWO-DIMENSIONAL DYNAMIC EXPERIMENTS ON OTTAWA SAND

A glass-sided container was constructed during the original contract period (11). This container was used during that program for five static loadings (G1-G5) and three series of dynamic loadings using dropped weights (G6-G8). Subsequent uses of this container have included footings on cohesive soil subjected to both static and dynamic loads (Appendix F) and slow rates of loading for footings on both dense and loose Ottawa sand (Appendix E).

This appendix reports on experiments of dynamically loaded footings on Ottawa sand. Since these experiments represent continuation of the original research using the glass-sided container (experiments No. G1-G8) the numbering system has been maintained. Table B-1 summarizes the experiments reported in this appendix. In every instance the footings involved are 3-in. wide and the soil is dry Ottawa sand. Movies of seven of the thirteen experiments have been provided in two reels, both of which have been supplied to the sponsor.

In the previous interim report on this project (12), sequence photos were presented in figure E-9 for a footing on dense Ottawa sand (Experiment No. G11) and in figure E-10 for a footing on loose Ottawa sand (Experiment No. G16). Figures B-1 and B-2 show sequence photos for footings on dense Ottawa sand subject to dynamic inclined (Experiment No. G19) and eccentric (Experiment No. G21) loads respectively.

Concentric vertical dynamic loads were applied by means of the pneumatic-hydraulic loading device discussed in Appendix A. For eccentric loads, the piston rod was simply located in the appropriate position on the footing. Special loading devices (Fig. B-3) were built for the inclined loads.

These devices assured application of the inclined load at the center of the bottom of the footing. Figure A-7 shows the experimental setup with dynamic loading apparatus placed to provide an inclined load.

The results of the two-dimensional dynamic experiments are shown in the photographs and movies obtained from the experiments. These pictures provide a qualitative understanding of footing behavior which is essential in attempting to develop improved analytical models to explain behavior of footing (8) when subjected to dynamic loads.

Table B-1

TWO-DIMENSIONAL EXPERIMENTS OF 3-IN. WIDE FOOTINGS ON OTTAWA SAND

Experiment No.	Average Density of Sand in Container (pcf)	Type of Load	Comments
G9	105.8	Vertical	Film 1
G10	108.5	Vertical	
G11	110.5	Vertical	Film 2
G12	110.0	Vertical	
G13	108.9	Vertical	
G14	108.8	Vertical	
G15	98.4	Vertical	Film 1
G16	98.5	Vertical	Film 1
G17	112.3	Eccentric (1/3 point)	
G18	120.5*	Eccentric (1/3 point)	
G19	111.1	Inclined (20° from vertical)	Film 2
G20	108.8	Inclined (20° from vertical)	Film 2
G21	109.2	Eccentric (1/3 point)	Film 2

*This value is unreasonable, and hence an error in the measurements or subsequent calculations must be assumed.

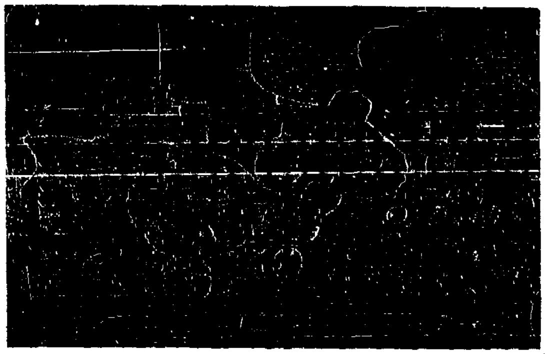

Start of Test

17 msec

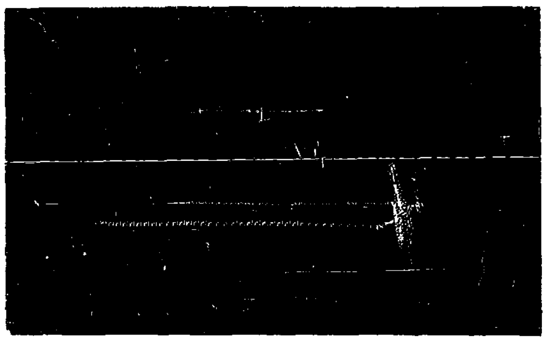

34 msec

52 msec

69 msec

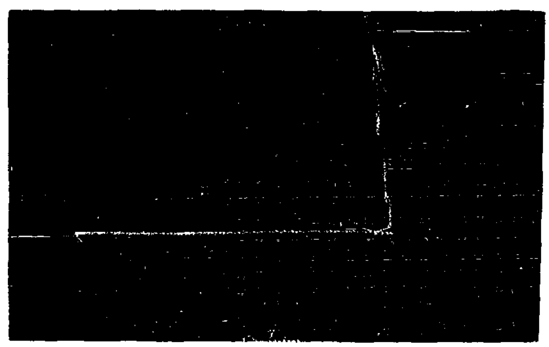

86 msec

Fig. B-1 SEQUENCE PHOTOS FOR INCLINED DYNAMIC LOAD ON FOOTING (Exper. No. G19)

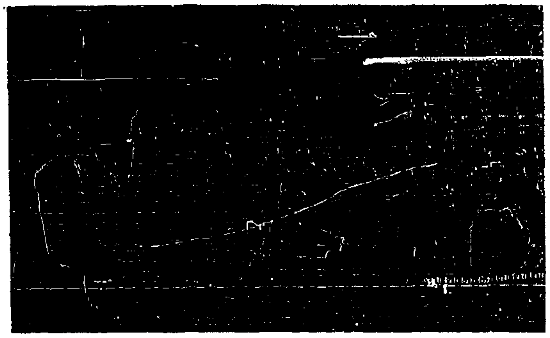

120 msec

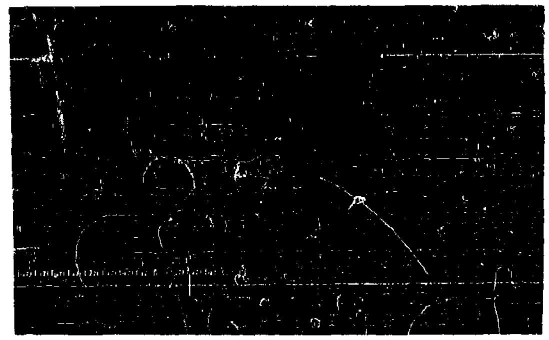

168 msec

End of Test

Fig. B-1 SEQUENCE PHOTOS FOR INCLINED DYNAMIC LOAD ON FOOTING (Cont'd)

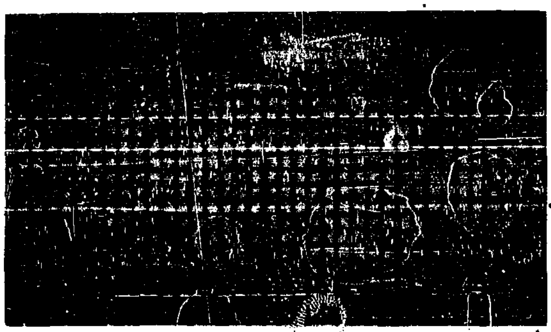

Start of Test

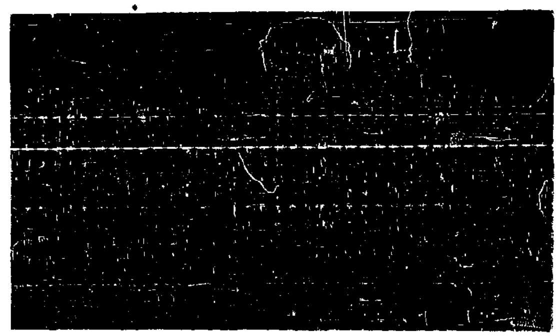

17 msec

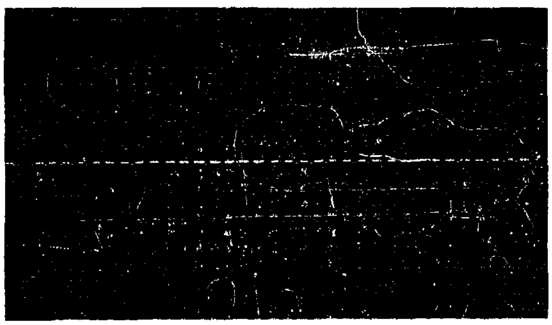

28 msec

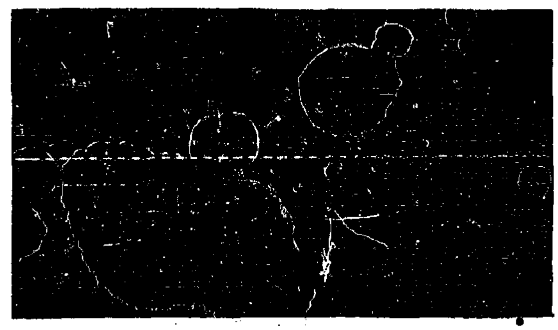

41 msec

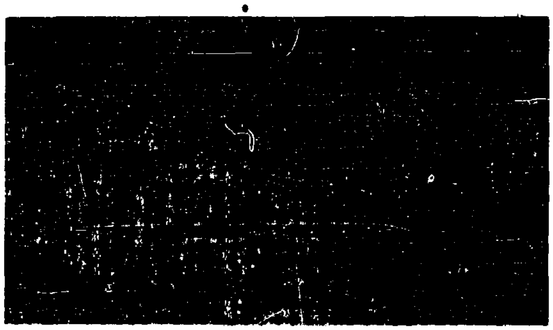

56 msec

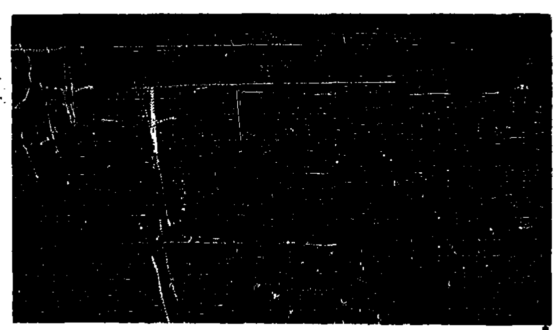

71 msec

Fig. B-2 SEQUENCE PHOTOS FOR DYNAMIC ECCENTRICALLY LOADED FOOTING
(Exper. No. G21)

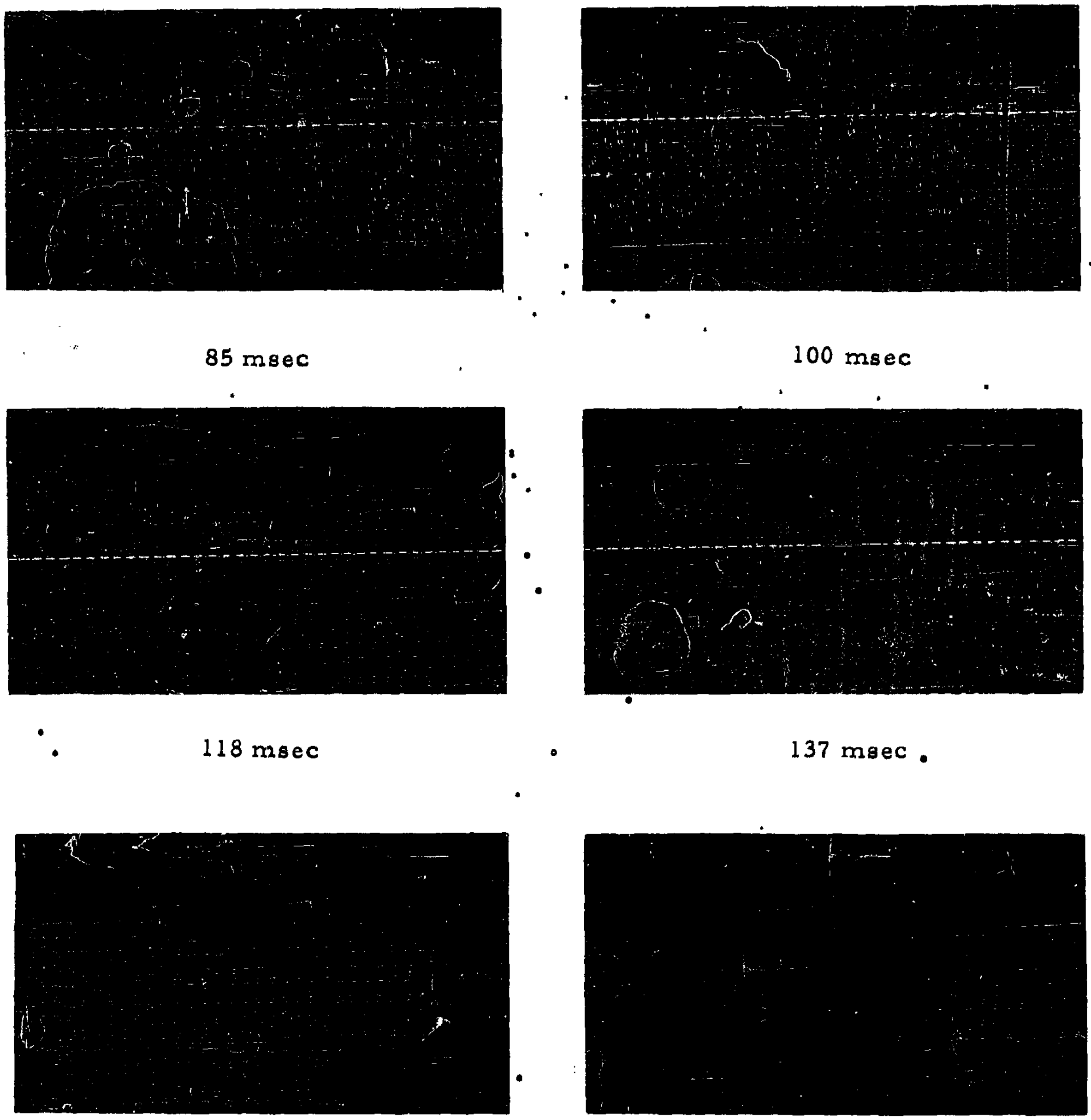

Fig. B-2 SEQUENCE PHOTOS FOR DYNAMIC ECCENTRICALLY LOADED FOOTING (Cont'd)

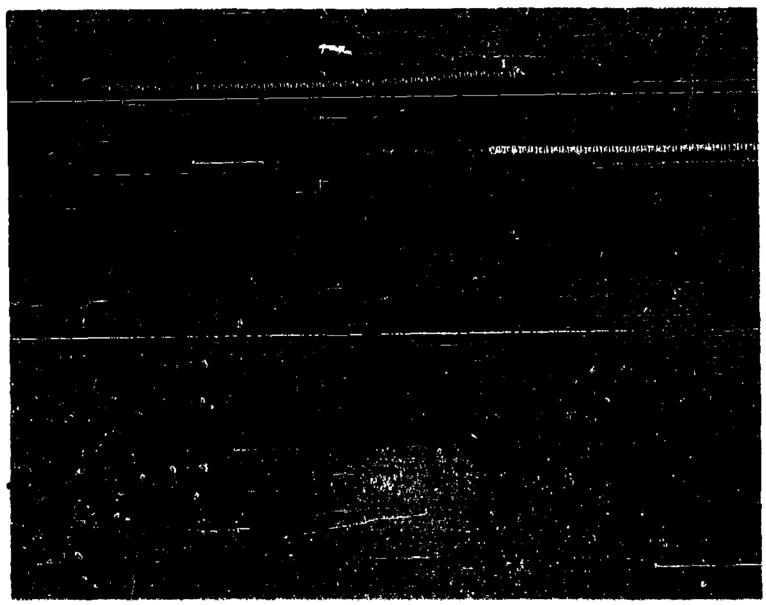

Fig. B-3 SPECIAL DEVICE FOR INCLINED LOADING

APPENDIX C

THREE-DIMENSIONAL DYNAMICALLY LOADED FOOTINGS

APPENDIX C

THREE-DIMENSIONAL DYNAMICALLY LOADED FOOTINGS

Three-dimensional studies were conducted in the sand box used during earlier research on this project.(9)(10). The box is approximately 4-ft square and 3-ft deep. The objective of this phase of the research was to obtain quantitative information regarding the behavior of small footings subjected to dynamic loads. The experiments reported herein were conducted on dense Ottawa sand. Two methods of load application were used in conjunction with the three-dimensional dynamic experiments; dropped weights and the ARF dynamic loader. For these experiments both the force-time history acting on the footing and the resulting displacement-time history of the footings were recorded. These experimental results are summarized in this appendix.

For reference, the experiments using a dropped weight were numbered sequentially with the original dynamic experiments (10) where dropped weights were used, i.e., D58 through D62. The experiments conducted in the sand box using the pneumatic-hydraulic loader were numbered P1 through P46.

Dropped Weights

The five dropped-weight loadings are summarized in table C-1. Figure C-1 shows a trace of a typical record for one of these experiments. As illustrated by this example, the measured peak force is extremely high and the time response relatively rapid. Actually, the measured response times were of the order of magnitude of the response time of the recording apparatus. Because of this limitation, the dropped-weight loadings were not quantitatively acceptable, and this phase of the experimental study was halted. Modification of the instrumentation system to permit accurate recording of the imposed force-time data was not felt to be justified within the realm of the present project; rather, it was felt that the technical effort would be more profitably, expended in experiments utilizing the pneumatic-hydraulic loading device.

Pneumatic-Hydraulic Loading

The ARF pneumatic-hydraulic loading system described in Appendix A, served as the primary method for applying dynamic loads. Table C-2 summarizes the results of these dynamic experiments.

The remaining experiments were conducted on 4-in. x 4-in. footings placed on the surface of dense Ottawa sand. Table C-2 lists the peak force and duration of the force, along with the maximum displacements observed on the records for each experiment. Figures C-2 through C-5 are typical records obtained for these experiments. Traces of the original records have been used for clarity and ease of reproducibility. These four records are typical and indicate the mode of behavior.

Table C-1

INSTRUMENTED DROPPED WEIGHT* LOADING

Experiment No.	Footing Size (in. x in.)	Weight Dropped (lb)	Peak Force (lb)	Duration** (msec)	Maximum Peak Displacement (in.)	Comments
D58	4 x 4	28.95	1390	13.9	0.051	
D59	4 x 4	28.95	1012	14.1	0.053	Peak force value is questionable.
D60	4 x 4	11.20	1064	6.6	0.003	
D61	4 x 4	11.20	1309	13.7	0.013	
D62	3 x 3	11.20	1417	11.6	0.045	

*All weights dropped from 5 inches.

**The duration is measured to the point where load reaches its static value.

Table C-2

DYNAMIC EXPERIMENT USING ARF PNEUMATIC-HYDRAULIC LOADER

Experiment No.	Footing Size (in. x in.)	Peak Force (lb)	Duration (msec)	Maximum Displacement (in.)	Time to Maximum Displacement (msec)
P1	4 x 4	366	>1000	>1	>64.0
P2	4 x 4	340	>1000	>1	>70.7
P3	4 x 4	303	1310	>1	>68.8
P4	4 x 4	277	249	0.989	82.1
P5	4 x 4	331	83	>1	>63.8
P6	4 x 4	394	70	>1	>66.2
P7	4 x 4	299	44	0.276	33.8
P8	4 x 4	137	25	0.044	15.2
P9	4 x 4	216	34	0.00	-
P10	4 x 4	397	54	0.29	50.9
P11	4 x 4	476	59	0.889	49.3
P12	30 in. diam.	434	57	-	-
P13	30 in. diam.	420	49	-	-
P14	30 in. diam.	430	57	-	-
P15	30 in. diam.	459	77	-	-
P16	30 in. diam.	462	79	-	-
P17	30 in. diam.	377	76	-	-
P18	30 in. diam.	531	61	-	-
P19	30 in. diam.	493	59	-	-
P20	30 in. diam.	194	58	-	-
P21		(Record spoiled)			
P22	30 in. diam.	203	85	-	-
P23	30 in. diam.	288	78	-	-
P24	4 x 4	324	24	0.16	17.3
P25	4 x 4	546	27	0.260	38.9
P26		(Record spoiled)			
P27	4 x 4	159	81	1.00	67.8
P28	4 x 4	148	69	0.937	59.8
P29	4 x 4	123	79	0.90	73.8
P30	4 x 4	168	66	0.932	56.9
P31	4 x 4	371	79	0.487	73.7
P32	4 x 4	112	87	0.151	
P33	4 x 4	104	81	0.046	42.2
P34	4 x 4	103	84	0.012	16.7
P35	4 x 4	104	70	0.012	14.0
P36	4 x 4	101	80	0.012	15.5
P37	4 x 4	140	71	0.012	15.3
P38	4 x 4	366	90	0.989	66.6
P39	4 x 4	334	73	0.893	62.9
P40	4 x 4	303	78	1.00	69.6
P41	4 x 4	272	72	0.957	66.4
P42	4 x 4	270	77	0.989	64.9
P43	4 x 4	272	84	0.152	64.3
P44	4 x 4	332	95	0.176	68.3
P45	4 x 4	341	122	0.150	71.2
P46	4 x 4	301	82	0.053	36.9

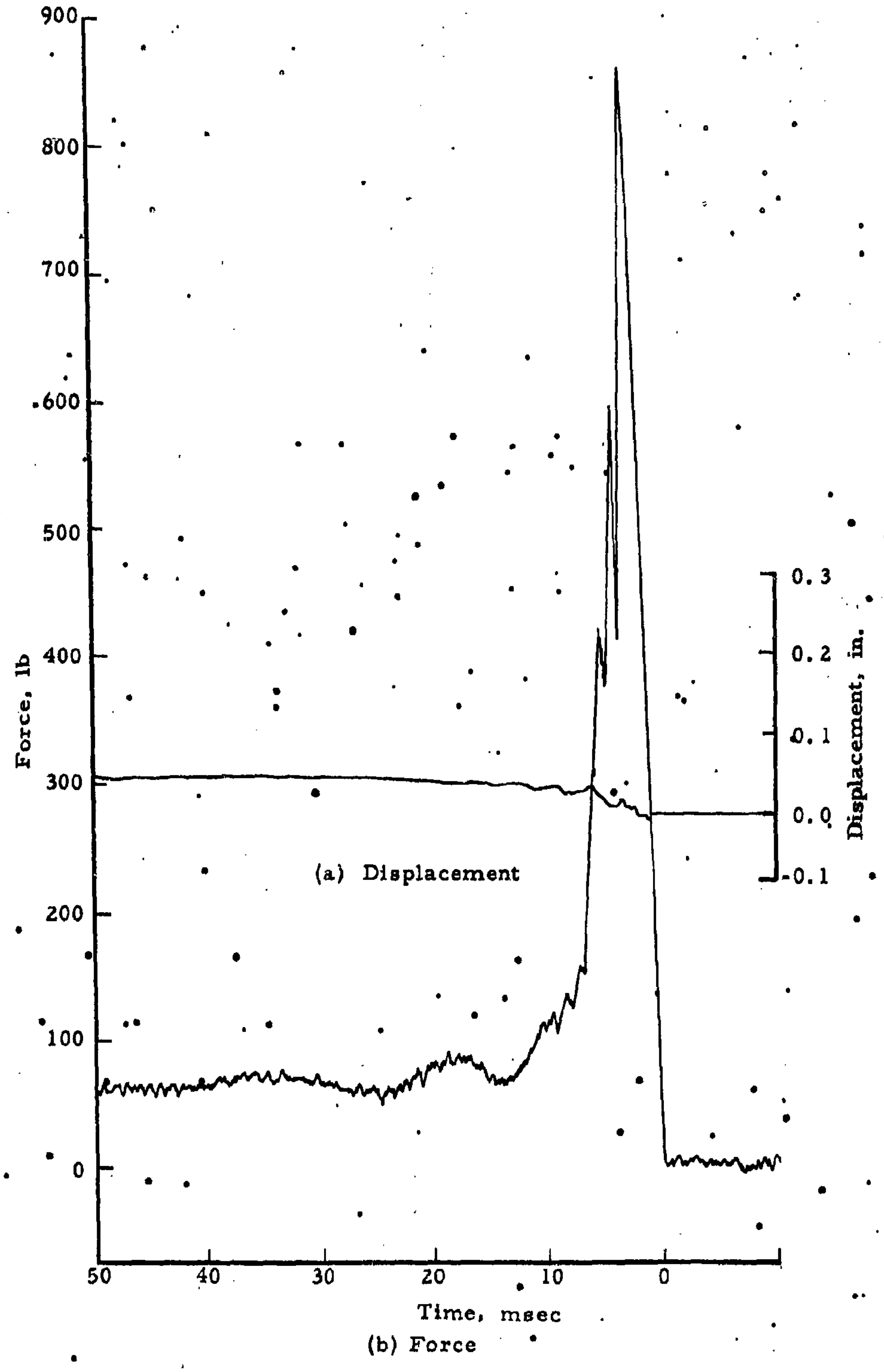

Fig. C-1 TYPICAL RECORD FOR DROPPED WEIGHT
(Exper. No. D59)

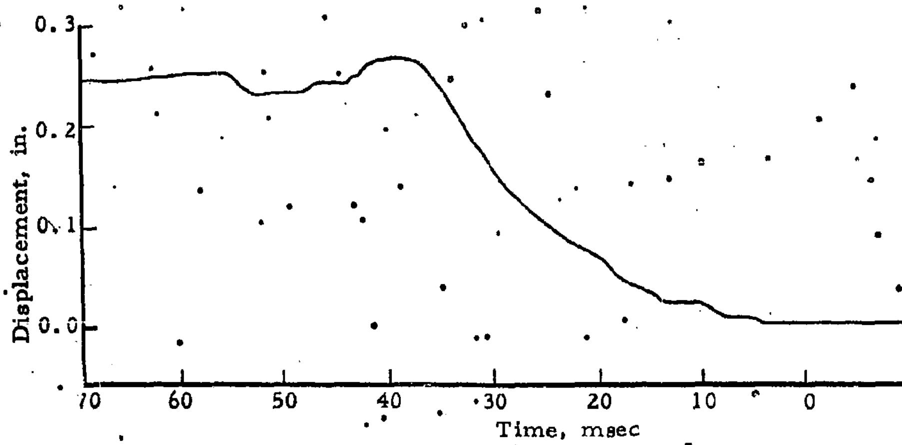

(a) Displacement

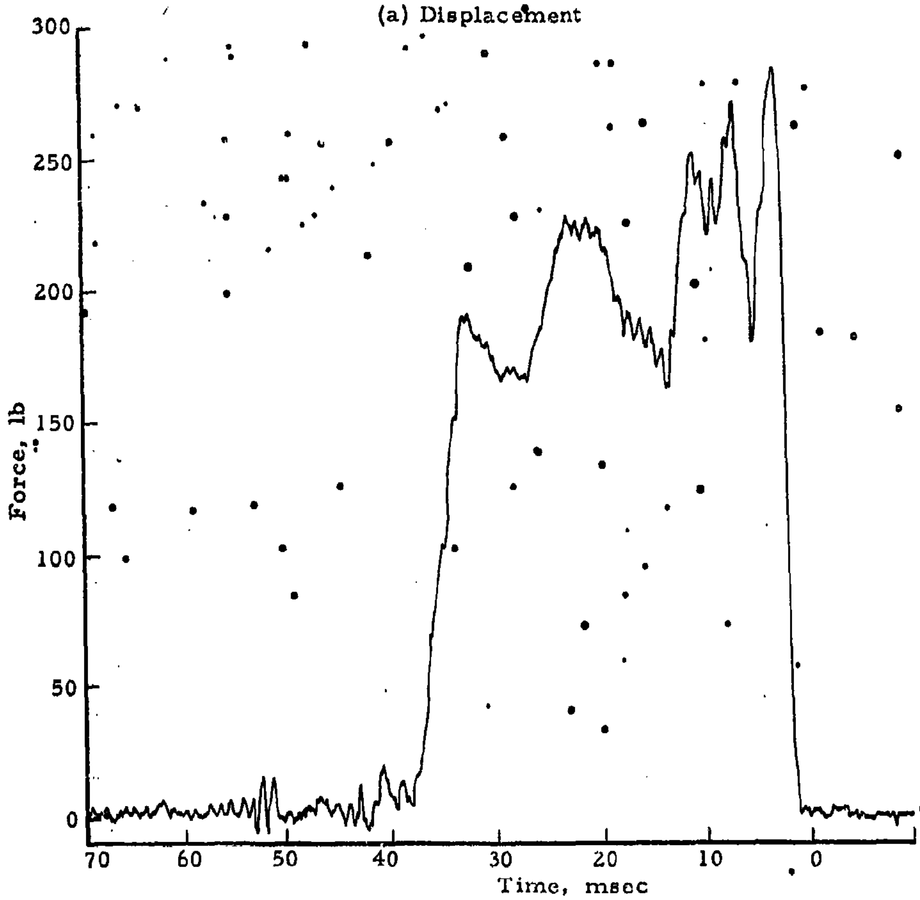

(b) Force

Fig. C-2 TYPICAL RECORDS FOR DYNAMICALLY LOADED FOOTING (Exper. No. P7)

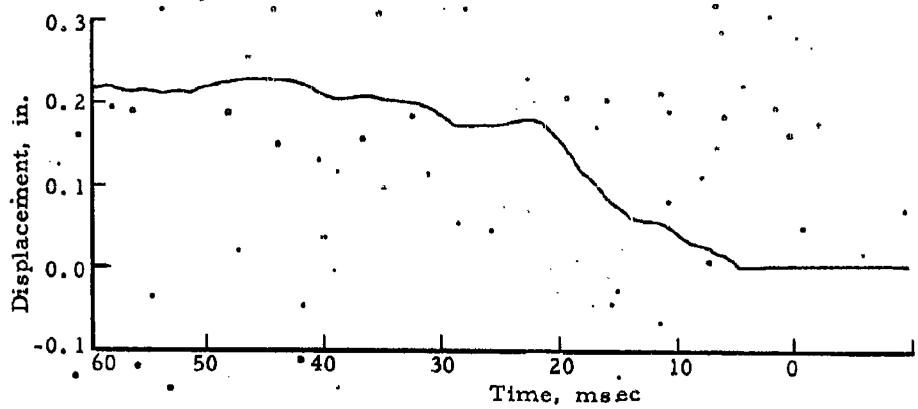

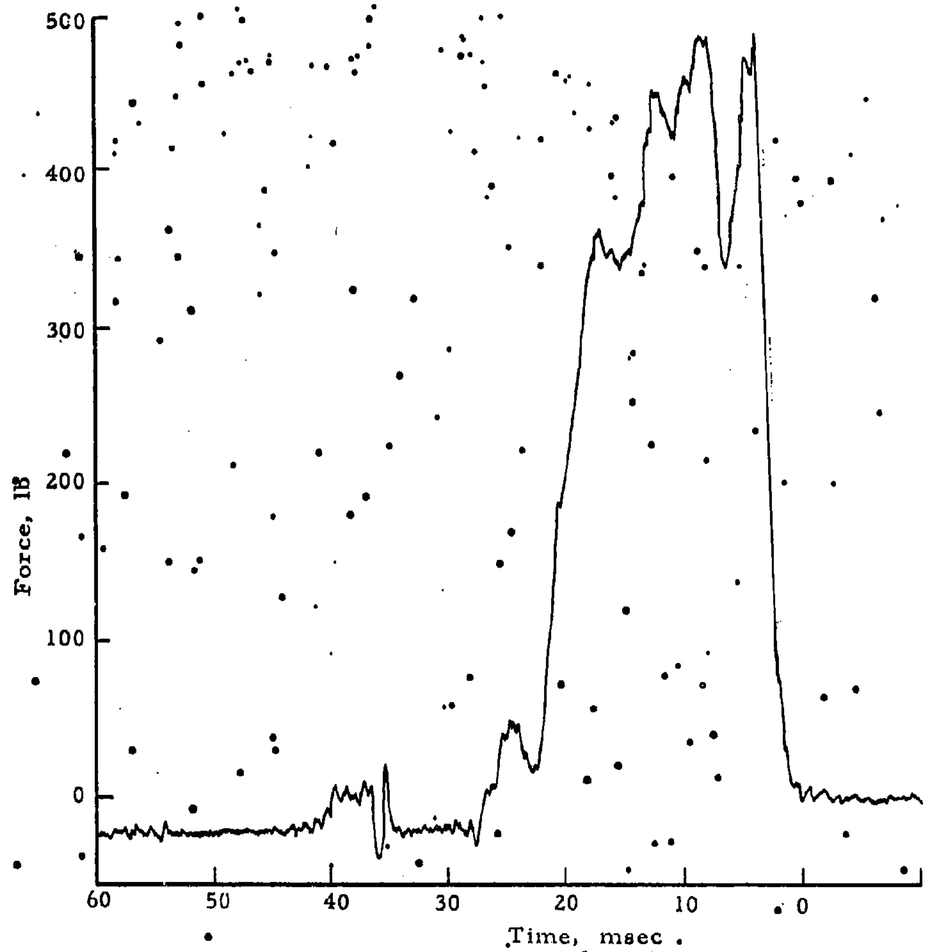

Fig. C-3 TYPICAL RECORDS FOR DYNAMICALLY LOADED FOOTING
(Exper. No. P25)

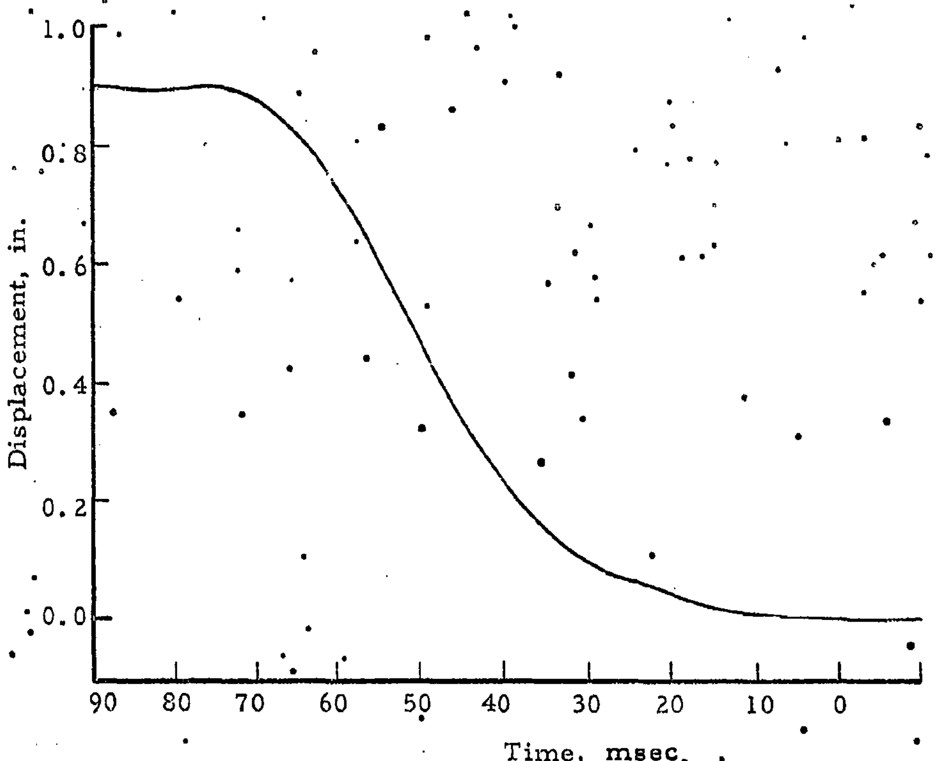

(a) Displacement

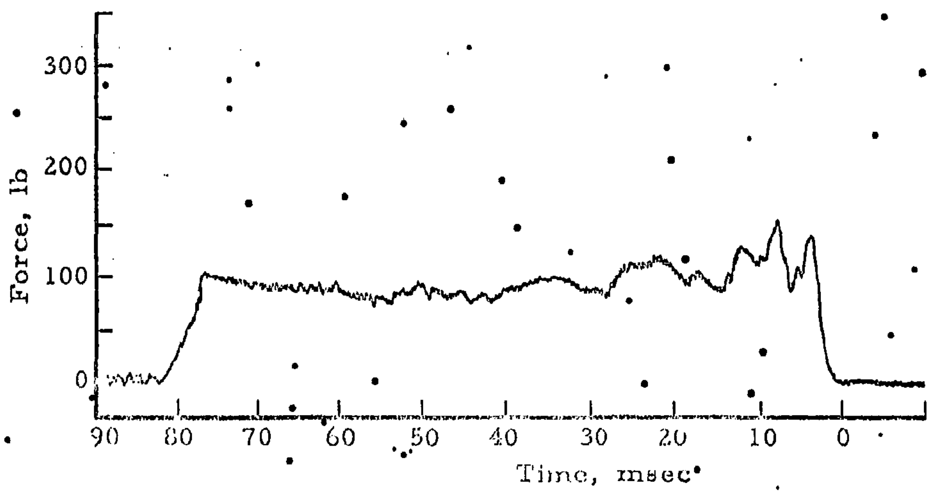

(b) Force

Fig. C-4 TYPICAL RECORDS FOR DYNAMICALLY LOADED FOOTING (Exper. No. P27)

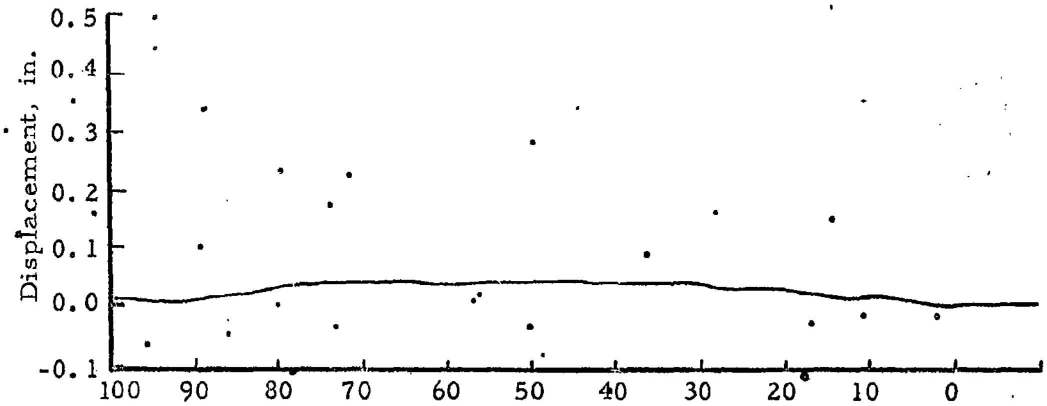

(a) Displacement

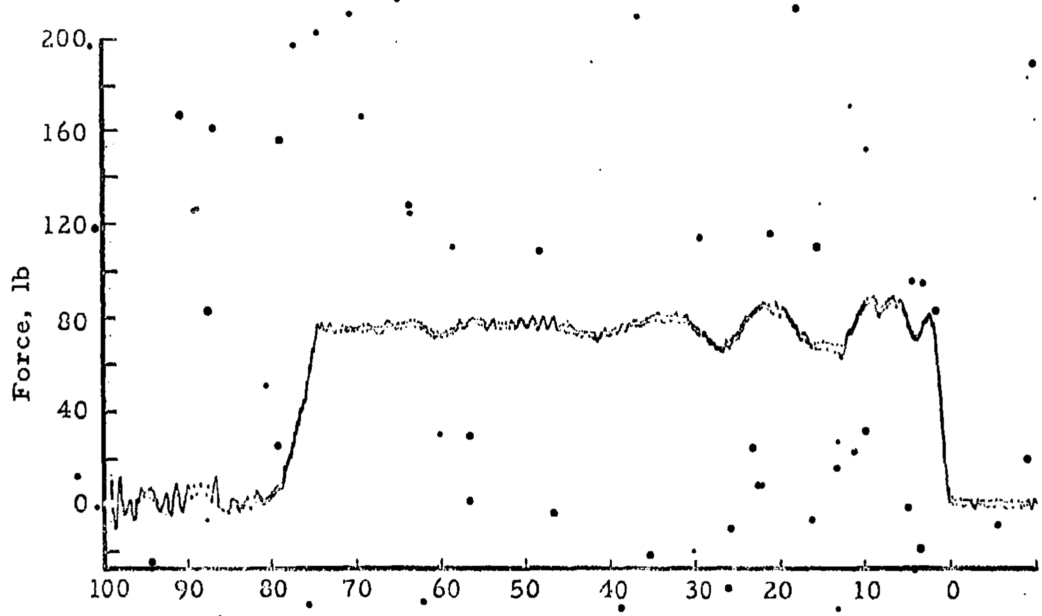

(b) Force

Fig. C-5 TYPICAL RECORDS FOR DYNAMICALLY LOADED FOOTING (Exper. No. P33)

APPENDIX D

FOOTINGS ON CALIFORNIA SAND

APPENDIX D

FOOTINGS ON CALIFORNIA SAND

During the original and current programs (8)(12) most of the experimental research has been done using dry Ottawa sand. Appendix F reports experimental studies in which cohesive soils were considered. This appendix reports on experiments using an alternate cohesionless material, referred to as California sand. This material was selected because it had been used in a series of dynamic plate bearing tests conducted in the blast simulator at the Naval Civil Engineering Laboratory, Port Hueneme, California. The sand was shipped from California specifically for use on this project.

Experiments using the California sand were limited to static loadings of three-dimensional footings in the sand box. The container had average base dimensions of 46.48 in. square. The sand was placed in the box in four layers, the bottom layer 12 in. the next two 6 in. and the top layer 6.56 in. Each layer was placed and vibrated uniformly over the proceeding layer for 20 minutes using a 1-hp flexible shaft concrete vibrator. The surface of each layer was then levelled and the weight of soil recorded. Surface densities were measured for each layer using the ARF density scoop (2). A sand sample was collected each time an additional three inches was added -- samples were combined for grain-size analysis and triaxial tests.

The average density of the sand based on measured weight and volume in the container was 105.0 pcf. The surface density of each layer after vibration was measured in four locations. These results were averaged and the average values are tabulated in Table D-1. In addition to the grain-size analyses of samples collected as the container was filled, subsequent grain size analyses were made on samples taken from the surface, a 12-in. depth, and a 24-in. depth in the container at the conclusion of the program (Fig. D-1).

Table D-1

AVERAGE DENSITY OF CALIFORNIA SAND

Layer No	Weight per Unit Volume, γ (pcf)
1	101.4
2	105.5
3	105.2
4	107.1

The line represents the average results of sieve analyses conducted on the samples obtained during placing. As indicated by the notation on the figure, the specific points are results obtained from samples from various depths within the container after the experimental program. Variations are within those anticipated from sample to sample; hence we conclude that repeated vibration caused no significant vertical migration of various grain sizes.

In an attempt to determine the soil properties six triaxial tests were conducted. The samples used had approximately 2.75-in. diameters and were eight inches high. The densities used were the highest that could be obtained in a cylinder of this size. The results of these triaxial tests are given in table D-2. Since there is no apparent correlation between the angle of internal friction and the density or lateral pressure, the average values of density and angle of internal friction were used. Based on the limited accuracy of the density determination and past experience dealing with triaxial tests of Ottawa sand (2) these values are assumed to give, at best, an indication of the correct value.

Experimental Results

The experimental techniques represent substantial refinements over those used previously on this program. Figure D-2 shows two photographs of the experimental setup. A gear box attached to the loading frame was used to apply loads to the proving ring. This load was transmitted to the footing through a ball bearing guide which guaranteed that there were no moments. The guide, along with the deflection gages, was supported on a plate which, in turn, rested on beams spanning the sand box. Deflections were measured at three points on the footing. In the following pages average values are used unless specifically stated otherwise. A grid of Ottawa sand spaced 5/8 in. center to center was placed on the surface to simplify observations of the surface behavior.

Table D-3 presents the results of this experimental series. For each experiment the footing size, bearing capacity, bearing pressure, and surface density are tabulated. Table D-4 presents the average values for each of the footing sizes included in the experimental series.

Figures D-3 and D-4 show the load-displacement curves for 4- and 5-in. square footings respectively. Figures D-5, D-6 and D-7 are photographs of typical footings after failure.

Analysis

Preliminary analysis of the experimental data indicated poor correlation. The reproducibility, as demonstrated in table D-4 by the variations in bearing capacities for the same size footing, is poor. Figure D-8 shows the ranges and average values for the three footing sizes. One would anticipate from available analysis that an inclined straight line should go through the origin. Such a straight line is drawn on the figure although the data would not justify this type of curve. When this was observed during the experimental portion of the program, a total of eight 3-in. x 3-in. footings were loaded in an attempt to improve the reproducibility. Considerable attention was devoted to improved controls on the placement techniques in order to increase the reproducibility. There was no noticeable improvement. At this stage, an investigation of the variations in soil properties was deemed necessary to explain the observed results.

Terzaghi's formula (18) for square surface footings on cohesionless soil is:

$$q_u = 0.4\gamma B N_\gamma, \qquad \text{(Eq. D-1)}$$

where:

q_u = bearing capacity for square footings, psi
γ = density of soil lb/in.^{3}
B = footing dimensions
N_γ = dimensionless factor depending on ϕ
ϕ = angle of internal friction.

A plot of N_γ versus ϕ is shown in figure D-9.

By applying equation D-1 to find N_γ and subsequently using figure D-9 to find ϕ, the experimental results presented in tables D-3 and D-4 can be used to determine ϕ. The values of ϕ would be 47° (with a range of 42.5 to 48°), 46° (with a range of 45° to 47°); and 45° (with a range of 44° to 46°) for 3-in., 4-in., and 5-in. square footings, respectively. If we consider the series of footings experiments as an involved method for determining ϕ, these results are quite consistent. The total range is 42.5° to 48° with an average value of about 46°. Comparison with the results of the triaxial test on the California sand (Table D-2) indicate that such results are reasonable for the soil densities found in the sand box.

The reason for the 'inconsistent' experimental results is now obvious. Relative minor variations in soil properties can make major differences in the bearing capacity. This is demonstrated by considering the pertinent portions of figure D-9. A change of 1° will produce a change of approximately 30% in the bearing capacity. Since no method of placing and compacting the soil between experiments is perfect, one must expect major variations between supposedly identical experiments when using a sand with a high value of ϕ.

The general shape of the load-deflection curves (Figs. D-3 and D-4) is of considerable interest. The first peak is associated with the bearing capacity and is the value discussed above. After this peak there is a decrease in load capacity and, with yet increased deflection, a rise to a second peak. For example, in Experiment No. C12 the first peak is 892 lb., a subsequent drop to 645 lb, and finally an increase to 1387 lb. For this 5-in. square footing, the second peak was 55% higher than the first and occurred at a displacement of 1.55 inch. Note also (Fig. D-4) that the load resistance at large displacements is fairly uniform for the different experiments while the bearing capacity is quite variable. The latter observation could reflect the changes in soil properties due to the loading (the properties approaching the same values independent of the initial conditions) or the influence of the footing displacement.

Table D-2

TRIAXIAL RESULTS

Density (pcf)	Lateral Pressure (psi)	Angle of Internal Friction ϕ (degrees)
106.8	10	41.1
102.5*	10	45.4
105.5	15	44.4
107.2	15	40.4
107.0	20	40.4
104.0	20	40.0
Average		
105.5		41.95

*There were large variations in the measurements of the diameter for this specimen and hence the density is of questionable accuracy.

Table D-3

STATICALLY LOADED FOOTINGS ON CALIFORNIA SAND

Experiment No.	Footing Size (in. x in.)	Bearing Capacity (lb)	Bearing Pressure (psi)	Surface Soil Density (pcf)
C1	3 x 3	132	14.7	107.1
C2	3 x 3	230	25.6	108.7
C3	3 x 3	256	29.5	*
C4	3 x 3	320	35.6	108.5
C5	3 x 3	350	38.9	*
C6	3 x 3	527.5	58.6	106.8
C7	3 x 3	506	56.2	108.1
C8	3 x 3	403	44.8	104.8 - 110.5
C9	4 x 4	965	60.3	107.1
C10	4 x 4	582	36.4	106.5
C11	4 x 4	730	45.6	106.4 - 107.7
C12	5 x 5	892	35.7	106.0 - 107.4
C13	5 x 5	930	37.1	108.3 - 109.3
C14	5 x 5	1502	60.0	108.7 - 109.9

*Surface density measurements not taken.

Table D-4

SUMMARY OF STATIC EXPERIMENTS ON CALIFORNIA SAND

Footing Size (in. x in.)	Average Density (pcf)	Average Bearing Capacity (lb)	Average Bearing Pressure (psi)
3 x 3	107.8	341.7	38.1
4 x 4	106.9	759.0	47.4
5 x 5	108.3	1108.0	44.3

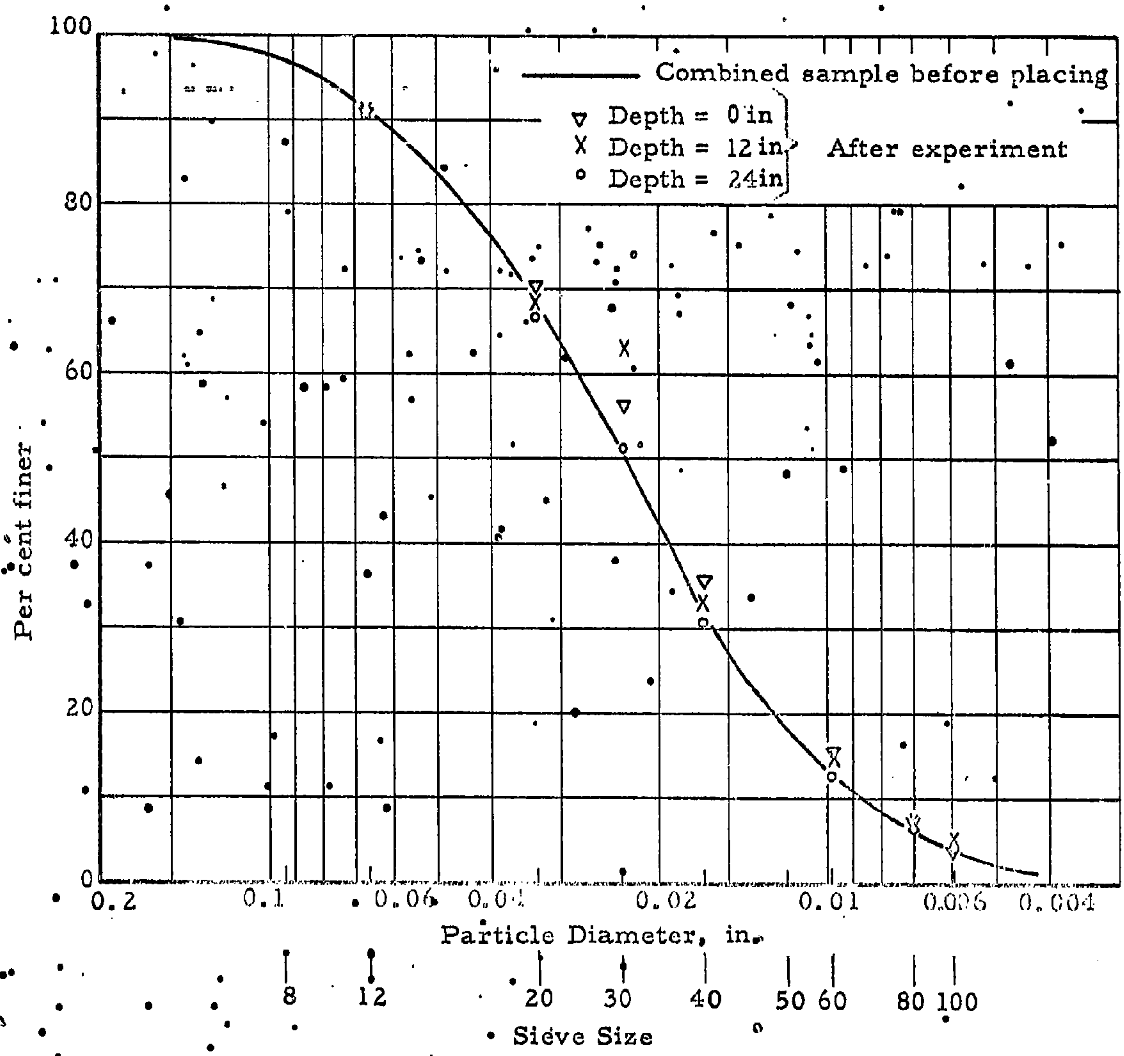

Fig. D-1 GRAIN SIZE DISTRIBUTION OF CALIFORNIA SAND

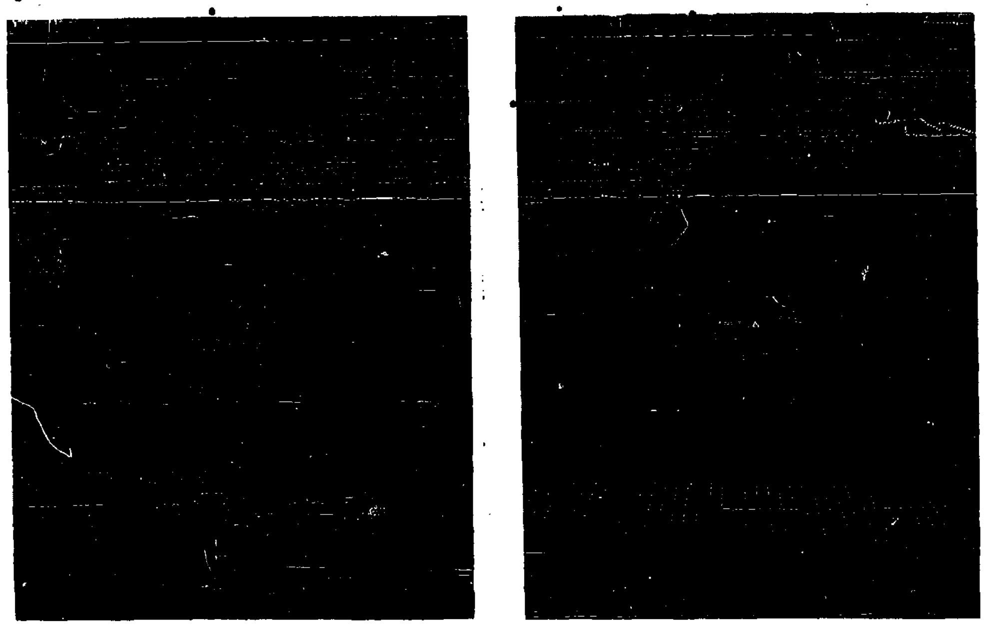

Fig. D-2 EXPERIMENTAL SETUP FOR CALIFORNIA SAND

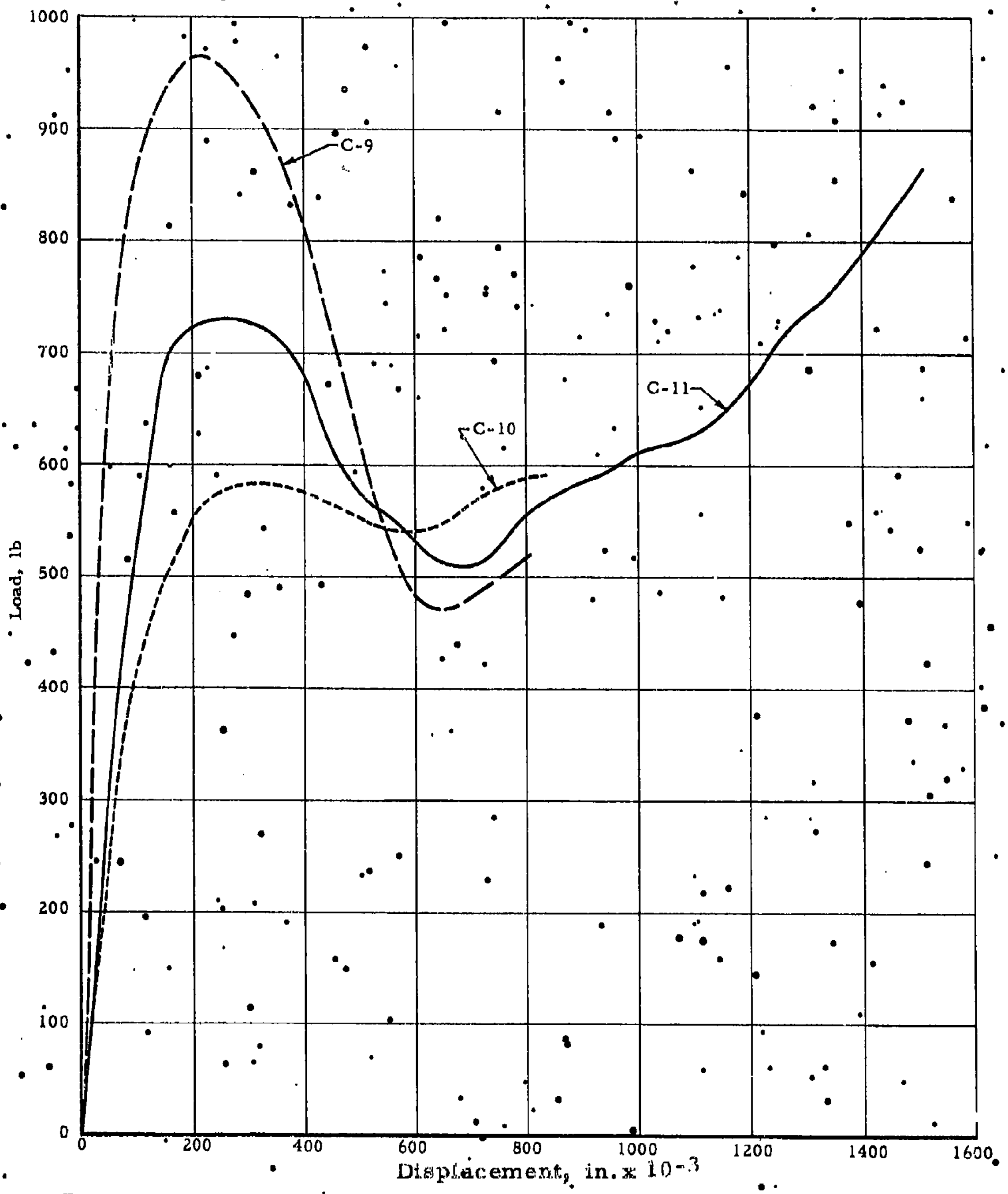

Fig. D-3 STATIC LOAD-DISPLACEMENT CURVES FOR 4-IN. SQUARE FOOTINGS ON CALIFORNIA SAND

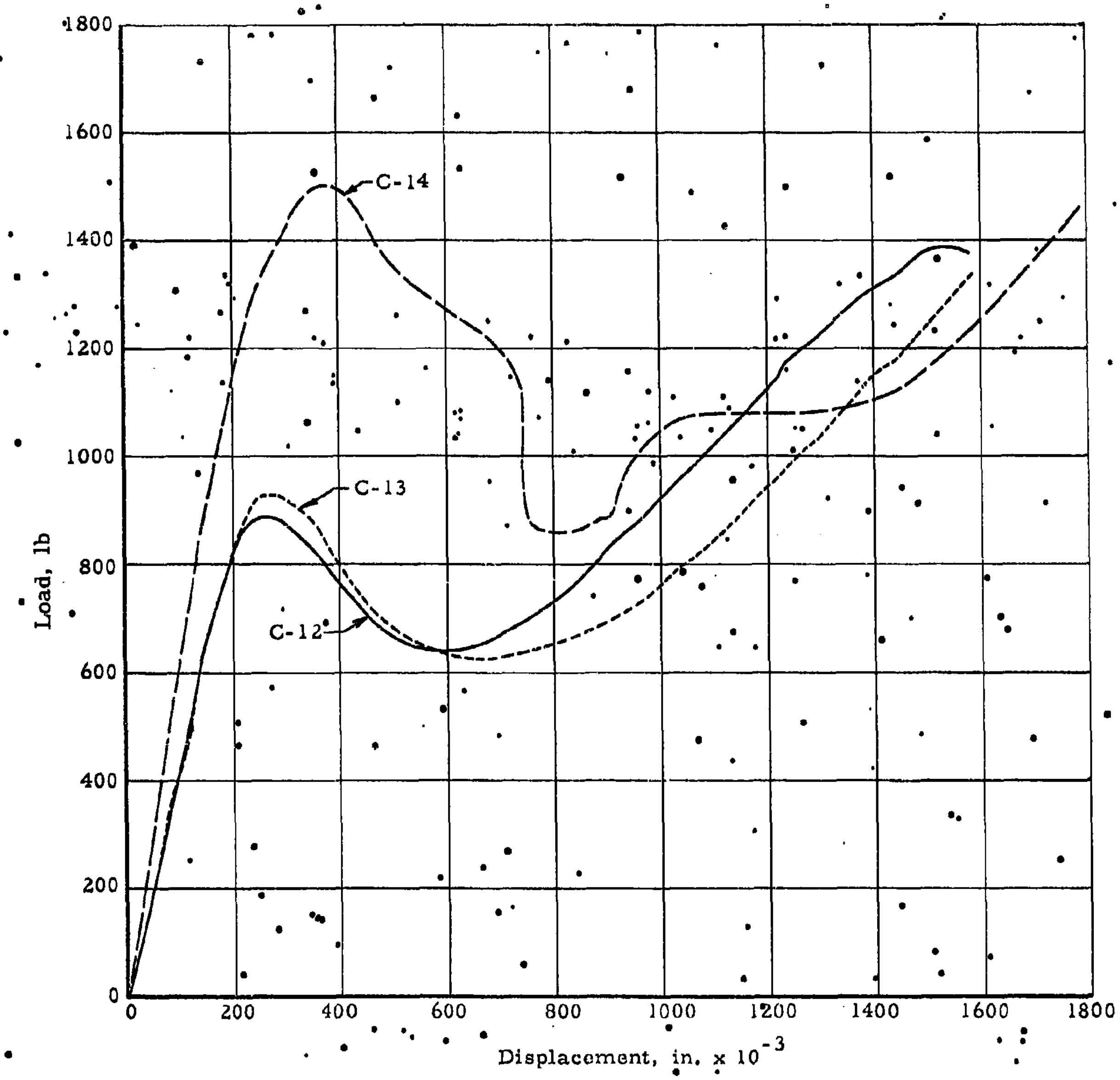

Fig. D-4 STATIC LOAD-DISPLACEMENT CURVES FOR 5-IN. SQUARE FOOTINGS ON CALIFORNIA SAND

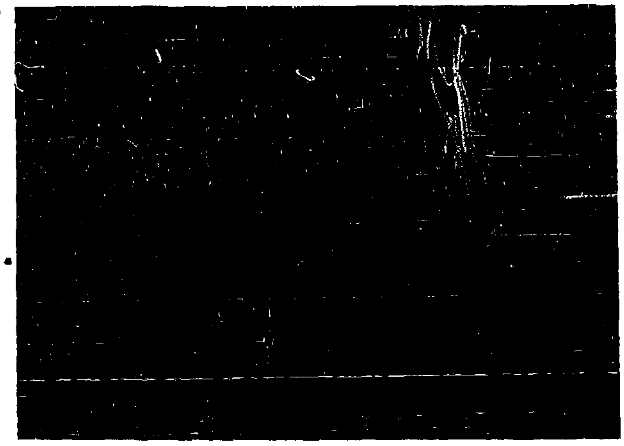

Fig. D-5 STATIC LOADING OF 3-IN. SQUARE FOOTING ON CALIFORNIA SAND (Exper. No. C-3)

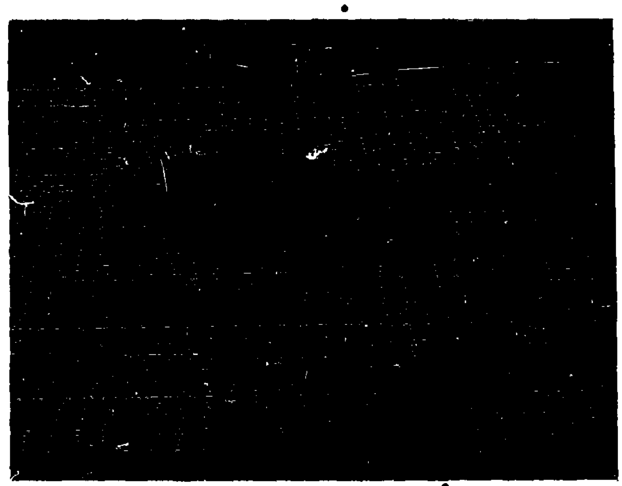

Fig. D-6 STATIC LOADING OF A 4-IN. SQUARE FOOTING ON CALIFORNIA SAND (Exper. No. C-11)

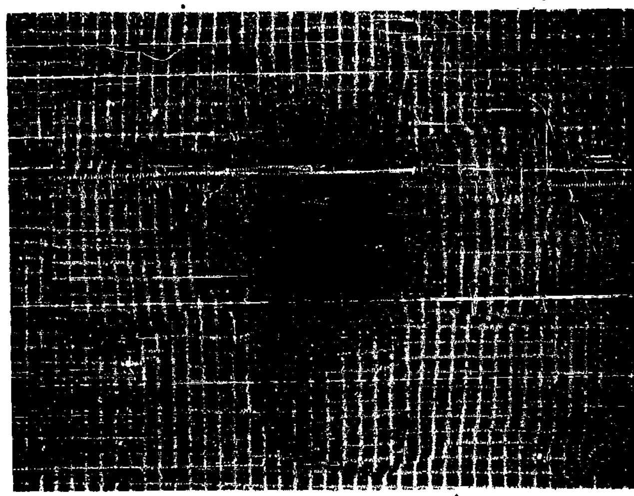

(a) Plan View

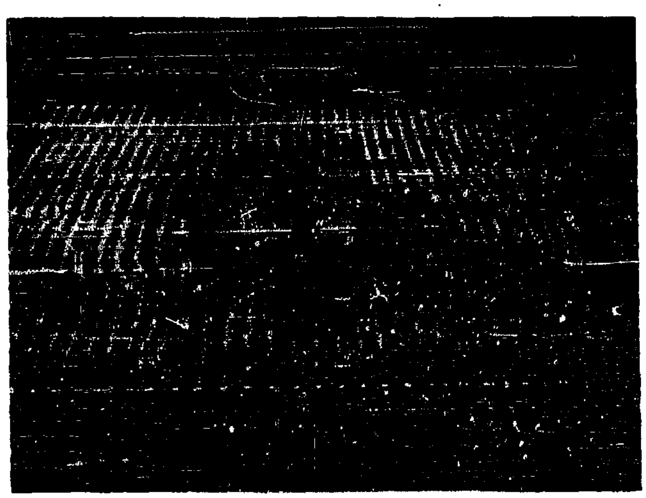

(b) Inclined View

Fig. D-7 STATIC LOADING OF A 5-IN. SQUARE FOOTING ON CALIFORNIA SAND

(Exper. No. C-14)

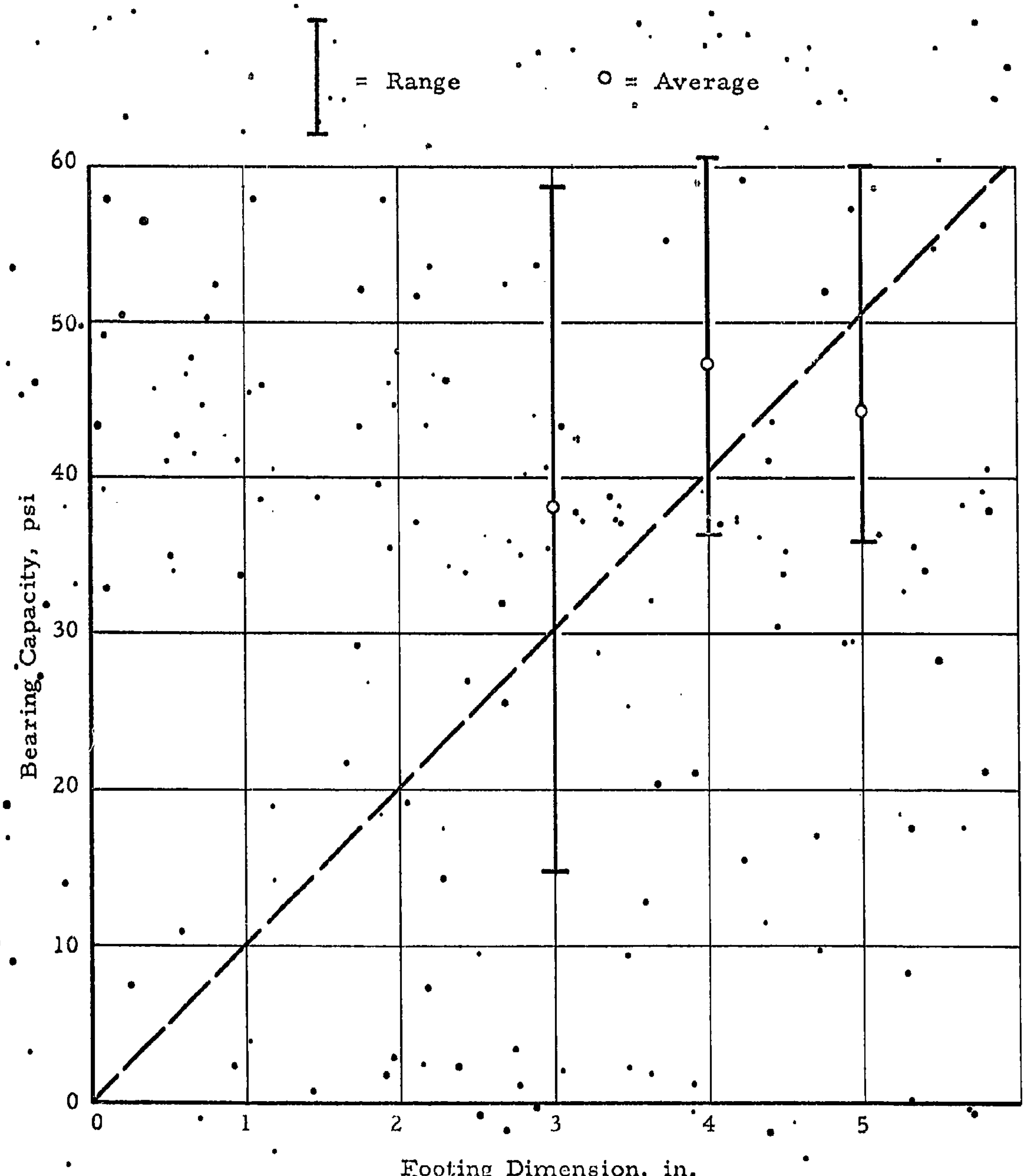

Fig. D-8 BEARING CAPACITIES VERSUS FOOTING DIMENSIONS

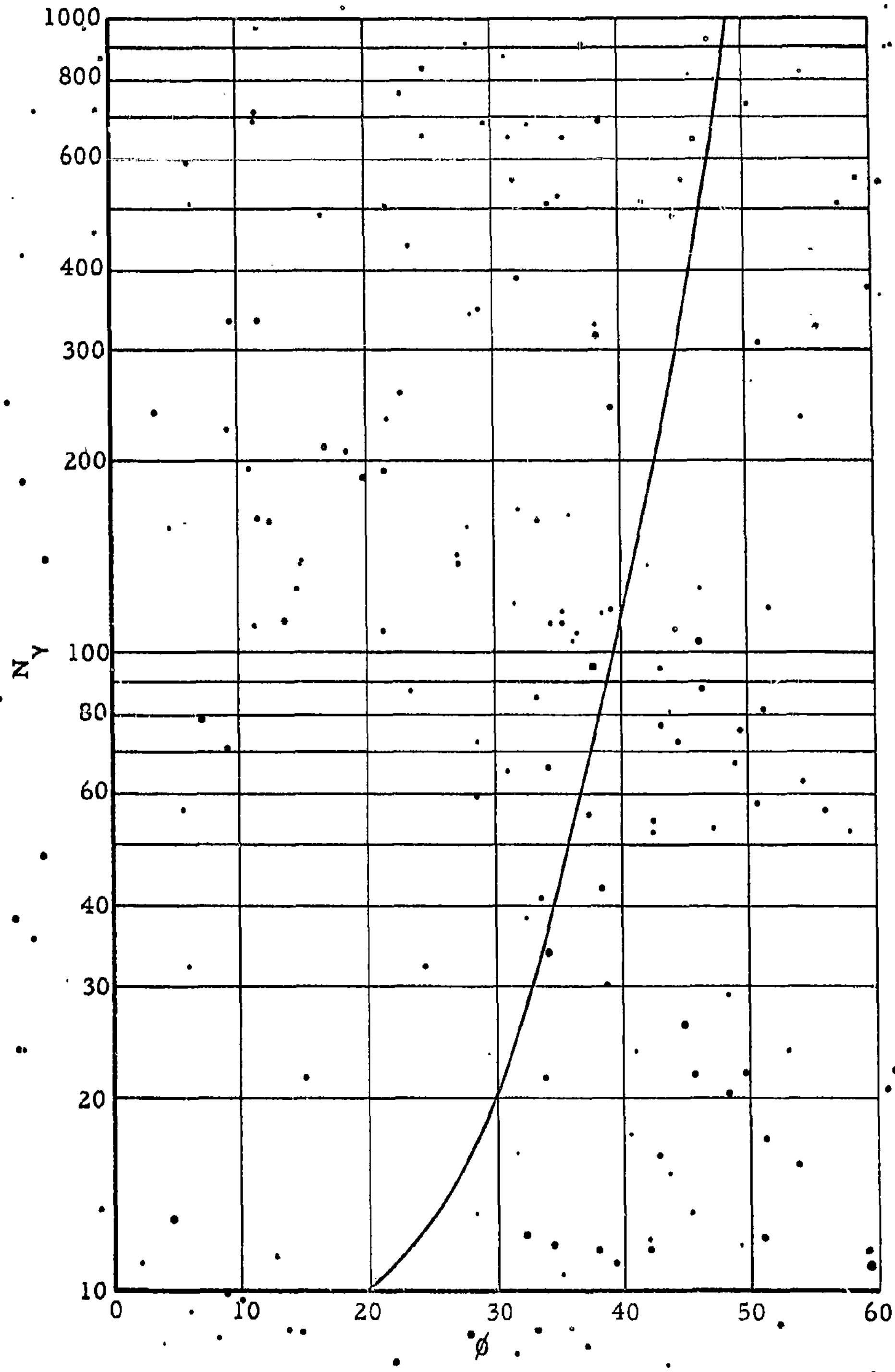

Fig. D-9 N_γ VERSUS ϕ

APPENDIX E

EFFECT OF LOADING RATE ON STATIC FOOTING BEHAVIOR

APPENDIX E

EFFECT OF LOADING RATE ON STATIC FOOTING BEHAVIOR

During the course of the over-all program, a large number of footings on sand were tested under "static" loading. There were questions raised as to whether, in fact, these loads were sufficiently slow to be considered static. The limited experimental program described herein was planned to investigate this question.

During early tests, static loads were applied through a hydraulic jack with the total load applied within five minutes. In more recent experiments, a gear box was used to apply the load. This arrangement allows control within reasonable limits of the rate of displacement to which the footings are subjected by controlling the number of turns per unit of time. By mechanically controlling this loading rate, it is possible to investigate the variations between "normal" and "slow" static loads. Consideration here was limited to cohesionless soils.

The previous report (13) on this project describes controlled loading rate tests for footings on both loose and dense sand. Two additional experiments were conducted to provide more complete data on footing behavior under controlled displacement (the downward speed of the top of the proving ring was kept at 0.00053 in. per minute). The load-deflection curves for dense and loose dry Ottawa sand respectively from these two experiments are shown on figures E-1 and E-2.

Figure E-1 for the dense Ottawa sand demonstrates the behavior associated with failure under static loads. Each point represents observed values; the straight lines connecting them, however, are approximations. Once significant displacement occurs (starting at approximately 100 lb) a repeated behavior is noted. The load increases with essentially no increase in displacement until suddenly there is a finite displacement and an associated reduction in load due to expansion of the proving ring. Under conditions for the controlled rate test, this stuttering is a very real phenomenon. With fewer observations the experimentalist could arrive at erroneous conclusions.

For a footing on loose sand (Fig. E-2) loaded in the same way with the same rate of load application (0.00053 in./min) the behavior is considerably different than for a footing on the dense sand. In general, there is a smooth curve relating the load and the displacement. Here again, all of the points shown are correct experimental points. The figure does show a limited number of points where decreases in the load were associated with increased displacements.

The jumping observed for the controlled rate of loading is undoubtedly a function of the rate of loading as well as the density of the sand. For the purposes of this project, it is sufficient to note that, in spite of the jumping, the values and general shape of the load-displacement curves for footings on dry Ottawa sand are the same for the controlled rate tests as for the hydraulically loaded footings tested in five minutes. It is, therefore, realistic to refer to footings on sand loaded by a hydraulic jack as statically loaded footings.

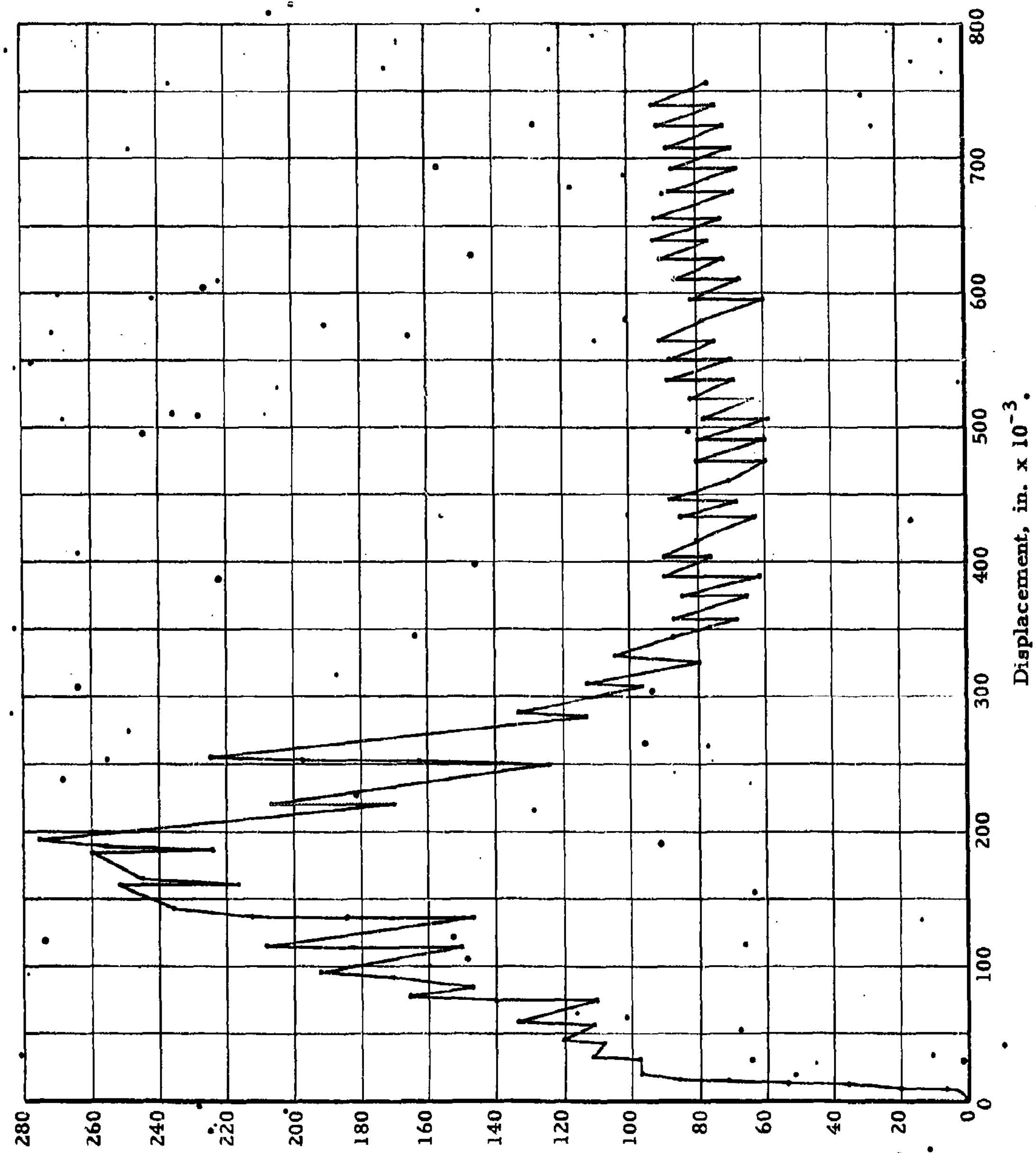

Fig. E-1 STATIC LOADING OF 3-IN. BY 4-IN. FOOTING ON DENSE OTTAWA SAND

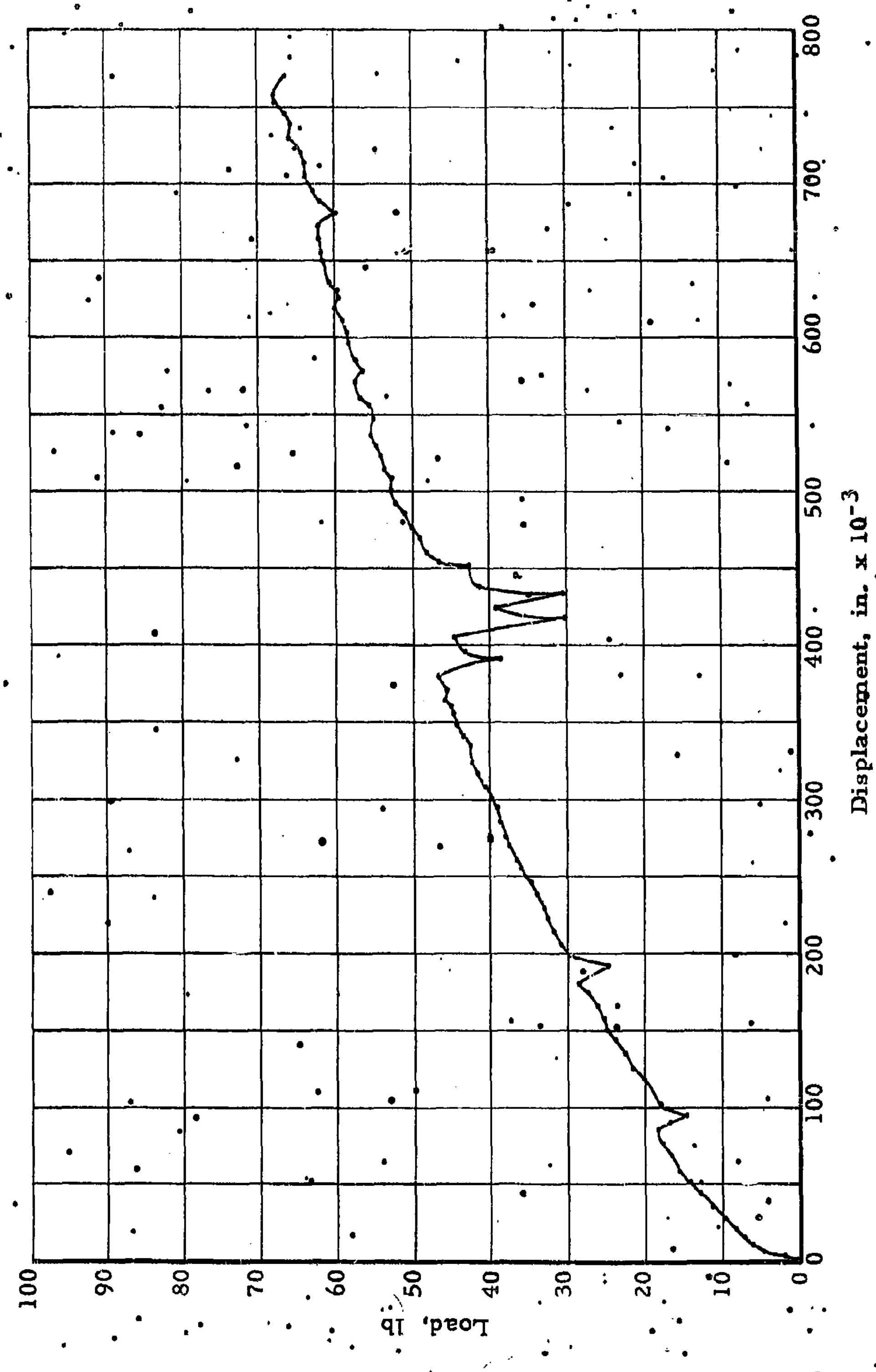

Fig. E-2 STATIC LOADING OF 3-IN. BY 4-IN. FOOTING ON LOOSE OTTAWA SAND

APPENDIX F

FOOTINGS ON COHESIVE SOIL

APPENDIX F

FOOTINGS ON COHESIVE SOIL

The major portion of the experimental studies conducted on this research program deals with footings on cohesionless soil. In an attempt to broaden the experimental basis of the project, a series of tests were conducted with footings on cohesive soil. This appendix describes these experiments which were conducted on footings subjected to both static and dynamic loads.

Laboratory studies on cohesive soils were limited to two-dimensional experiments conducted in the glass-sided container. The decision to consider only two-dimensional footings on cohesive soils was based on a number of factors including: (i) the relatively small size of the glass-sided container simplifies the problems involved in soil placement, (ii) two-dimensional studies allow more complete observation; and (iii) two-dimensional experiments are more directly comparable with available theoretical solutions. The undesirable feature introduced by limiting consideration to two-dimensional footing is that the resulting data will be of limited quantitative accuracy due to the edge effects on the two sides.

The initial construction of the two-dimensional container was described in an earlier report on this project (11). In connection with the experiments involving cohesive materials, substantial modifications of this container were required because of the much increased loading. Essentially, it was necessary to strengthen the glass sides. This may be done in three ways: by introducing an intermediate steel member to reduce the span of the glass, by replacing the ordinary glass with tempered glass, or by replacing the glass sides by steel plates during load application. All three of these techniques were used during the course of the present study. It should be noted that since the two-dimensional container attempts to simulate the plane strain situation the sides ideally should be rigid. Obviously this ideal is satisfied to a greater or lesser extent depending on the rigidity of the sides.

Another modification to the glass-sided container was the incorporation of a double thickness of glass enclosing a plastic sheet marked with grid-lines. These grids, which match those initially placed on the soil specimen, provide a reference against which to observe soil movements.

Compaction of the cohesive soils in the two-dimensional container was the subject of considerable investigation. A standard mechanically-operated compaction machine (Soiltest Model CN422), designed to compact soil into a 1/30-cu ft cylindrical mold, was enlarged and modified to compact cohesive soil mixtures into the container to a depth of 18 inches. The circular hammer was replaced by a 10-lb rectangular hammer (4 in. x 2 in.) that closely fit the wall dimensions of the model box. A roller base was added that enables the container to be passed under the hammer in indexed increments until a complete layer of soil was compacted. By varying the number of layers and number of blows per layer, a given soil density was obtained. The compactor mechanism always raised the hammer 12 in. above the surface of the soil during the entire filling of the container. A photograph of this setup is included as figure F-1.

As will be observed in later photographs of the experimental results (Fig. F-4), in most instances, failures took place along the boundary between compacted layers. The appearance of this effect was reduced by increasing the number of layers (using thinner layers) and decreasing the number of blows per layer. Nevertheless, so long as the soil is placed and compacted in horizontal layers, one would expect the soil properties to reflect the method of placement. As a matter of fact, even in nature, the properties must reflect the placement which implies a layered effect. This is undoubtedly a broad field for soil mechanics research, but for our purposes the objective was only to avoid obvious discontinuities between the layers. No attempt was made to establish the effect such discontinuities might have on the soil properties.

All of the footing experiments connected with cohesive soil are reported in this appendix. To assure uniformity and reproducibility, the cohesive materials used for these investigations were manufactured in the laboratory from basic constituents. The results of an ARF sponsored program (15) were used in selecting the constituents used. Tables F-1 through F-3 present data for the soil constituents which are used. For a more complete discussion of the manufactured soil, the reader is referred to the ARF research.

Static Experiments

A series of four preliminary experiments was conducted using a manufactured soil of fire clay, Ottawa sand, and mineral oil. The particular mixture has many questionable features because of the oil base. However, in establishing procedures for placement and testing, the oil base offers distinct advantages since it is little influenced by exposure to the atmosphere and hence can be reworked and retested with only negligible variations in its properties. The data from these four tests were not assumed to have quantitative significance.

Table F-4 summarizes these four experiments. The solid materials used in putting together this soil were 50% air-floated ball clay (95% Kaolinite) and 50% uniform Ottawa sand (20-40 Mesh). Light mineral oil (DTE 150), equal to 22.1% of the total dry weight, was added and the constituents mixed uniformly. Because the mineral oil does not evaporate, this mixture remained unchanged during its usage (15). The soil properties of this mixture are not discussed, since there is no attempt to use these results in a quantitative fashion.

Knowledge obtained from these preliminary loadings led to increasing the strength of the container, decreasing the density (weakening) of the soil, and decreasing the width of the footings.

Figures F-2 and F-3 show typical experimental results for cohesive soils. This preliminary work was followed by a series of nine static tests. The soil used for these tests was ball clay (95% Kaolinite) mixed with various quantities of water. For all practical purposes, although it was manufactured, this is a natural soil, since it consists only of a natural constituent (ball-clay) and water. Because it is manufactured from controlled materials, one might anticipate better reproducibility and greater control, but fundamentally it is no less 'real' than a specimen removed from the ground and remolded. Compaction was carried out in the same manner as described for the artificial soils. Since placement of the specimen represents a major problem, four of the five specimens were reused by removing the disturbed portion of the soil and conducting a second experiment on the remaining soil.

Table F-5 summarizes this series of nine static-footing experiments. The letter 'A' after an experiment number indicates the second loading using the same soil specimen. The specimens for later experiments were prepared using more layers with a reduced number of blows per layer.

During the course of this experimental work, special care was taken to minimize loss of moisture. Two dishes of water were suspended near the top of the soil container and the container sealed. The success of these precautions is demonstrated by one of the dynamic experiments in which the soil specimen stood for one week with a change in moisture content of approximately 1%.

Figures F-4 and F-5 are photographs of two of these static loadings. Figure F-4 shows experiment No. 3 with pronounced layer effects. Figure F-5 shows experiment No. 5A where the improved placement had reduced the layered effects. The results of the experiments listed in table F-5 are summarized in table F-6. Figures F-6 and F-7 are typical plots of the load displacement curves for footings on cohesive soil.

Dynamic Experiments

A series of six dynamic experiments was performed for footings on cohesive soil. Table F-7 summarizes the results of this laboratory research. Fig. F-8 shows experiment No. 7 where the footing has been punched.

into the soil much as one would expect for a pile. Fastax films of this failure are available on loan upon request to the sponsor. The soil used for these experiments was the fire clay-water mixture discussed in connection with the static studies.

The first five dynamic tests were performed on a single container of soil. The full container had a moisture content ranging from 21.1 to 22.0%, with a wet density of 128.5 pcf. The first four loadings were performed on this soil. Experiments No. 6 and 6A produced no observable displacement while the movies indicated at the most "elastic" behavior for 6B. After one week, the moisture content was found to be 20.2 to 20.7%. Experiment No. 6C was performed on this soil. The disturbed portions of the soil were removed and experiment No. 6D conducted. The moisture content after the loading was found to be 20.2%.

The final test, experiment No. 7, was performed with a 1-in. wide footing on a soil having a density of 127.8 pcf and an average moisture content of 24%. Figure F-8 shows the results of this experiment.

Comparison with Theory

It is interesting to compare the maximum resistance from the static experiments with the predictions which result from direct application of the bearing capacity formulas for two-dimensional footings. The maximum bearing for a footing on a purely cohesive soil woud be:

$$q = 5.70\ c \qquad \text{(Eq. F-1)}$$

where:

q = bearing capacity

c = cohesion, psi.

The maximum force the footing can resist, P_s, is given by

$$P_s = 5.70\ cA, \qquad \text{(Eq. F-2)}$$

where A is the area of the footing.

As part of the ARF sponsored study of artificial soils (15) the unconfined compressive strength was determined for several values of the moisture content and maximum obtainable density. (A curve of this data is included as figure F-9.) For cohesive materials the unconfined compressive strength, q_u, is equal to twice the cohesive strength. Hence equation F-2 can be written in terms of the unconfined compressive strength as

$$P_s = 2.85\, q_u A. \qquad \text{(Eq. F-3)}$$

Considering the nine static experiments reported in tables F-5 and F-6, experimental results can be compared with theoretical predictions (Table F-8). In determining the unconfined compressive stress the average moisture content from table F-5 was used. The area for each of the footings was 10 sq inches.

For most of the experiments, the comparison of theory with experimental data was disappointing. As indicated by table F-8, the theory in 8 out of 9 cases gave results over 50% less than the experimental values. There are at least two possible reasons for this discrepancy: (i) the experiments are not truly two-dimensional since the friction between the soil and the container sides add to the resistance, and (ii) the soil in the container was at a much greater density than samples used for unconfined compressive tests and hence would be expected to be a "stronger soil". Both of these factors are undoubtedly present and contributing to the poor comparison. This assumes the theory to be correct. There is always a certain skepticism regarding the theories, but in this instance, the experiments appear to be responsible for most of the variations.

A number of other considerations regarding experimental and analytical approaches could be introduced, but seem irrelevant to this study. Both static and dynamic tests of small footings conducted in the laboratory have given useful results both quantitatively and qualitatively. The experimental difficulties encountered are understandable and could be overcome in future work. For example, in testing three-dimensional footings, effects caused by the container sides can be eliminated. At any rate, the results of these pilot experiments are encouraging and will aid in conducting future experiments with cohesive soil.

Table F-1

CHARACTERISTICS OF KAOLIN

Name:	Florida plastic kaolin.	
Supplier:	Edgar Plastic Kaolin Co., Edgar, Florida.	
Source:	Edgar, Florida.	
Mineral Content:	Better than 99% kaolinite.	
Preparation:	Airfloated.	
Chemical Analysis:	Aluminum Oxide	38.71 %
	Silicon Dioxide	45.91
	Iron Oxide	0.42
	Titanium Dioxide	0.34
	Calcium Oxide	0.09
	Magnesium Oxide	0.12
	Sodium Oxide	0.04
	Potassium Oxide	0.22
	Ignition Loss	14.16
		100.00 %
Atterberg Limits:	Liquid Limit = 70.2, Plastic Limit = 40.8 Plasticity Index = 29.4, Shrinkage Limit = 22.8	
Particle Size:	30-40 micron	2 %
	20-30	2
	10-20	4
	5-10	10
	3- 5	11
	2- 3	11
	1- 2	12
	1/2-1	10
	Less than 1/2 micron	38
		100 %
Specific Gravity:	2.66	
Color:	White.	

Table F-2

CHARACTERISTICS OF BALL CLAY

Name:	OM 4 Kentucky ball clay.
Supplier:	Kentucky-Tennessee Clay Co., Mayfield, Ky.
Source:	Kentucky old mine 4.
Mineral Content:	Approximately 75% kaolinite with the remainder illite, montmorillonite, feldspar, and quartz.
Preparation:	Airfloated.
Chemical Analysis:	Silicon Dioxide 51.72 %
	Aluminum Oxide 31.98
	Titanium Dioxide 1.52
	Iron Oxide 0.87
	Calcium Oxide 0.21
	Magnesium Oxide 0.19
	Potassium Oxide 0.89
	Sodium Oxide 0.38
	Ignition Loss 12.24
	100.00 %
Atterberg Limits:	Liquid Limit = 62.6, Plastic Limit = 31.3 Plasticity Indix = 31.3, Shrinkage Limit = 21.6.
Specific Gravity:	2.69.
Color:	Tan when dry, medium brown when wet.

Table F-3

CHARACTERISTICS OF OTTAWA SILICA SAND

Name:	Ottawa flint shot silica sand.
Supplier:	Ottawa Silica Co., Ottawa, Illinois.
Source:	St. Peter sandstone, Ottawa, Illinois.
Mineral Content:	Better than 99% silica (SiO_2).
Preparation:	Sandstone is blasted and mined. The sand is then washed to remove the clay present and graded to the desired size ranges.
Particle Size:	98% between 0.84 mm and 0.42 mm.
Specific Gravity:	2.65.
Color:	Off-white.
Comments:	Well-rounded particles.

Table F-4

PRELIMINARY STATIC EXPERIMENTS

Experiment No.	Footing Size (in. x in.)	Soil Density γ (pcf)	Peak Force (lb)	Deflection at Peak Force (in.)	Comments
Y1	3 x 4	121.0	930	0.52	Glass broke
Y2	3 x 4	117.2	1625	1.31	Load released at 930 lb, glass sides replaced by steel. Load reapplied and released at 1430 lb. Load reapplied and released. Deflection reduced to 1.25 in. when load was released.
Y3	3 x 4	111.0	1000	0.94	Deflection reduced to 0.86 in. when load released.
Y4	2-1/2 x 4	112.5	1260	1.55	Deflection reduced to 1.46 in. when load released.

Table F-5

STATIC EXPERIMENTS

Experiment No.	Moisture Content w (%)	No. of Layers	Blows per layer	Footing Size (in. x in.)	Density γ (pcf)	Comments
1	17.5 to 18.5	6	30	2-1/2 x 4	118.0	
2	20.2 to 21.4	8	75	2-1/2 x 4	131.0	
2A	20.6 to 21.0			2-1/2 x 4		
3	21.1 to 21.7	10	60	2-1/2 x 4	128.0	
3A	21.1 to 21.7			2-1/2 x 4		6 in. removed from original sample
4	21.4 to 23.2	36	15	2-1/2 x 4	121.5	
4A	21.3 to 25.2			2-1/2 x 4		One-Half depth of original sample removed
5	20.6 to 22.1	40	16	2-1/2 x 4	129.0	
5A	20.2 to 21.9			2-1/2 x 4		Original sample cut down to undisturbed soil

Table F-6

STATIC EXPERIMENTS

Experiment No.	Footing Size (in. x in.)	Peak Force (lb)	Deflection at Peak Force (in.)	Final Deflection (in.)	Force at Final Deflection (lb)
1	2-1/2 x 4	1130	1.75	1.95	900
2	2-1/2 x 4	815	0.69	1.13	555
2A	2-1/2 x 4	775	0.45	0.87	715
3	2-1/2 x 4	668	0.64	1.42	172
3A	2-1/2 x 4	735	0.50	1.12	243
4	2-1/2 x 4	1000	0.67	1.42	470
4A	2-1/2 x 4	807	0.50	1.33	560
5	2-1/2 x 4	925	0.63	0.73	910
5A	2-1/2 x 4	905	0.50	0.70	640

Table F-7

DYNAMIC EXPERIMENTS

Experiment No.	Moisture Content w (%)	Unit Weight γ (pcf)	Footing Size (in. x in.)	Line Pressure (psi)	Peak Force Based on Line Pressure (lb)	Comments
6	20	128.5	3 x 4	1000	783	No permanent deflection
6A	20	128.5	3 x 4	1400	1100	No permanent deflection
6B	20	128.5	2 x 4	1350	1060	Slight deformation in elastic behavior
6C	20	128.5	1 x 4	1250	983	Footing failed
6D	20	128.5	1 x 4	1200	943	Footing failed
7	24	127.8	1 x 4	1000	783	Failed by punching like pile

Table F-8

COMPARISON OF EXPERIMENTAL WITH THEORETICAL RESULTS

Experiment No.	Moisture Content w (%)	Unconfined Compression Stress, q_u (psi)	Peak Force (lb)	Calculated Strength (lb)	Variation (%)
1	18.0	40.0	1130	1140	0.9
2	20.8	13.5	815	385	52.8
2A	20.8	13.5	775	385	50.3
3	21.4	12.2	668	348	47.9
3A	21.4	12.2	735	348	52.7
4	22.3	10.9	1000	311	68.9
4A	23.2	9.8	807	279	65.4
5	21.3	12.2	925	348	62.4
5A	21.0	13.0	905	370	59.1

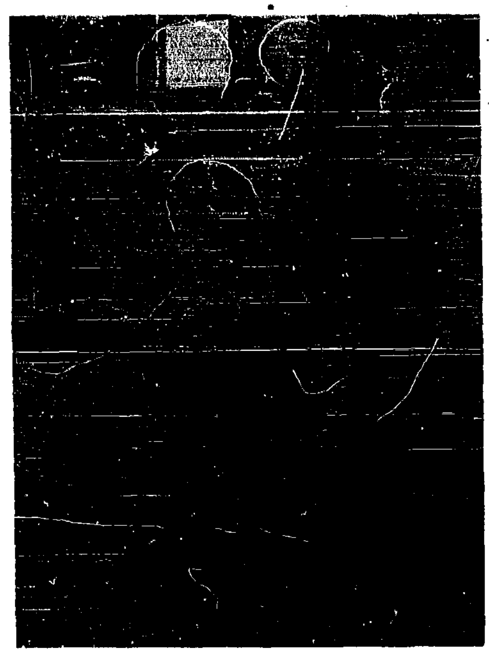

Fig. F-1 COMPACTER MODIFIED FOR USE IN COMPACTING COHESIVE MATERIAL IN GLASS BOX

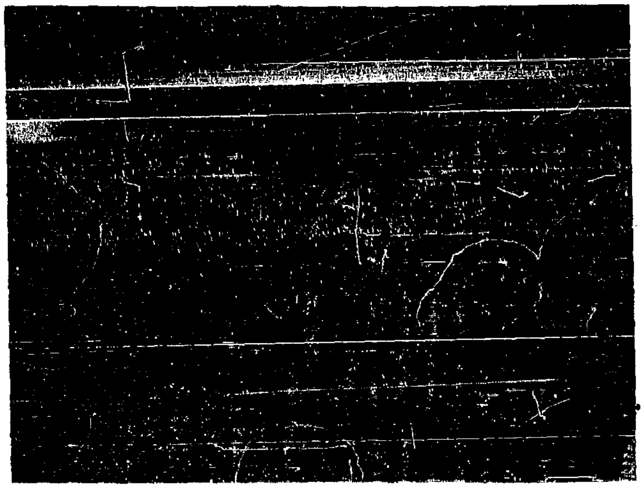

Fig. F-2 EXPERIMENT NO. Y3 AFTER STATIC LOADING

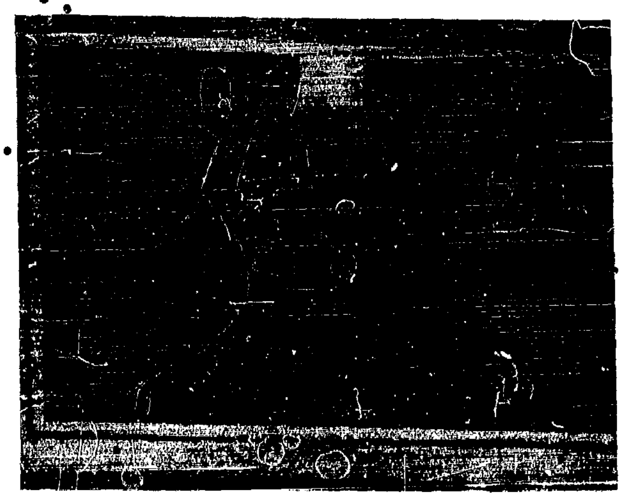

Fig. F-3 EXPERIMENT NO. Y4, 1-1/2 IN. DEFLECTION

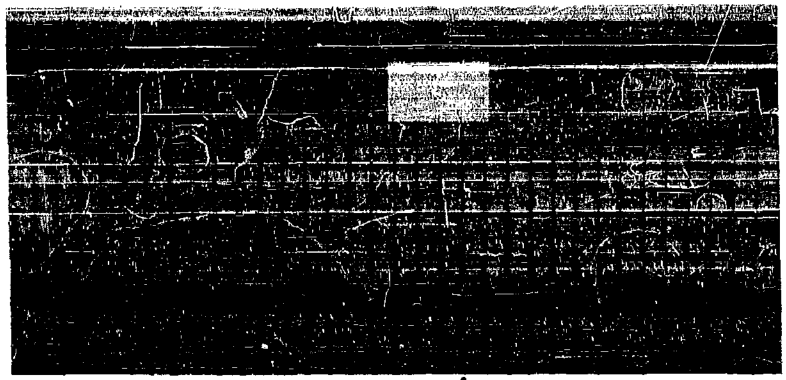

(a)

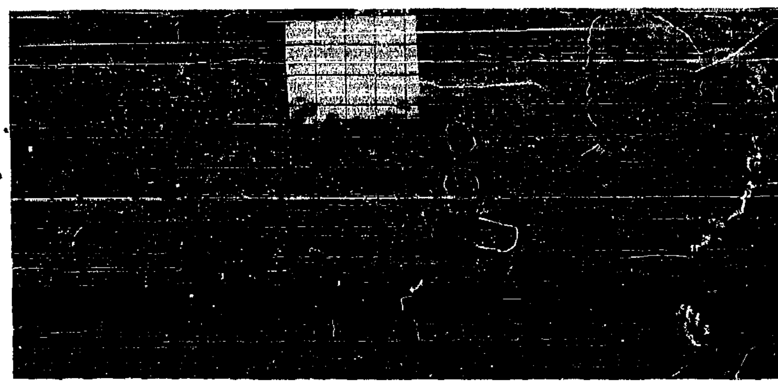

(b)

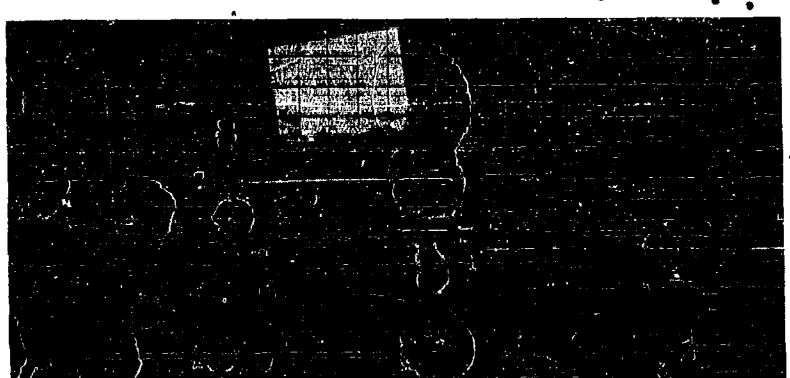

(c)

Fig. F-4 PROGRESSIVE FAILURE OF COHESIVE SOILS (Exper. No. 3)

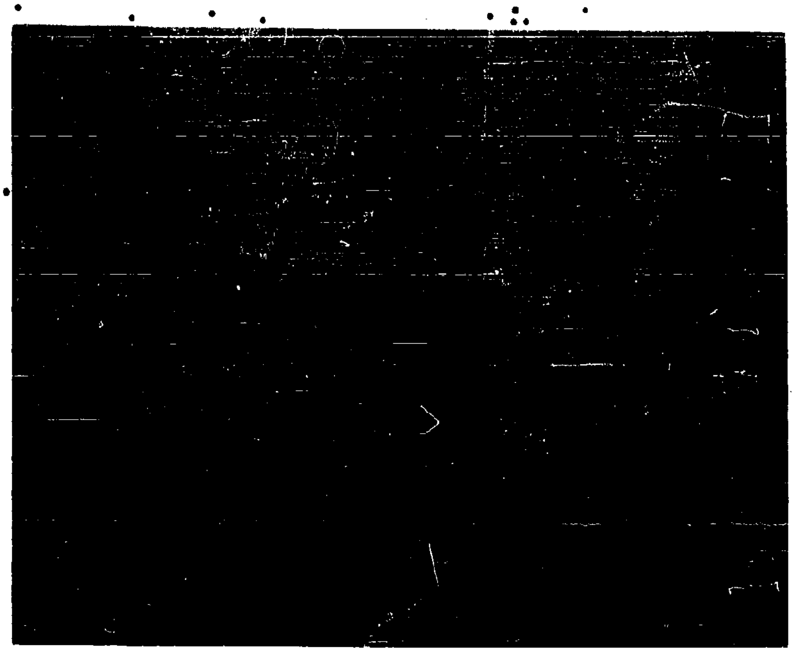

Fig. F-5 FOOTING ON COHESIVE SOIL AFTER FAILURE
(Exper. No. 5A)

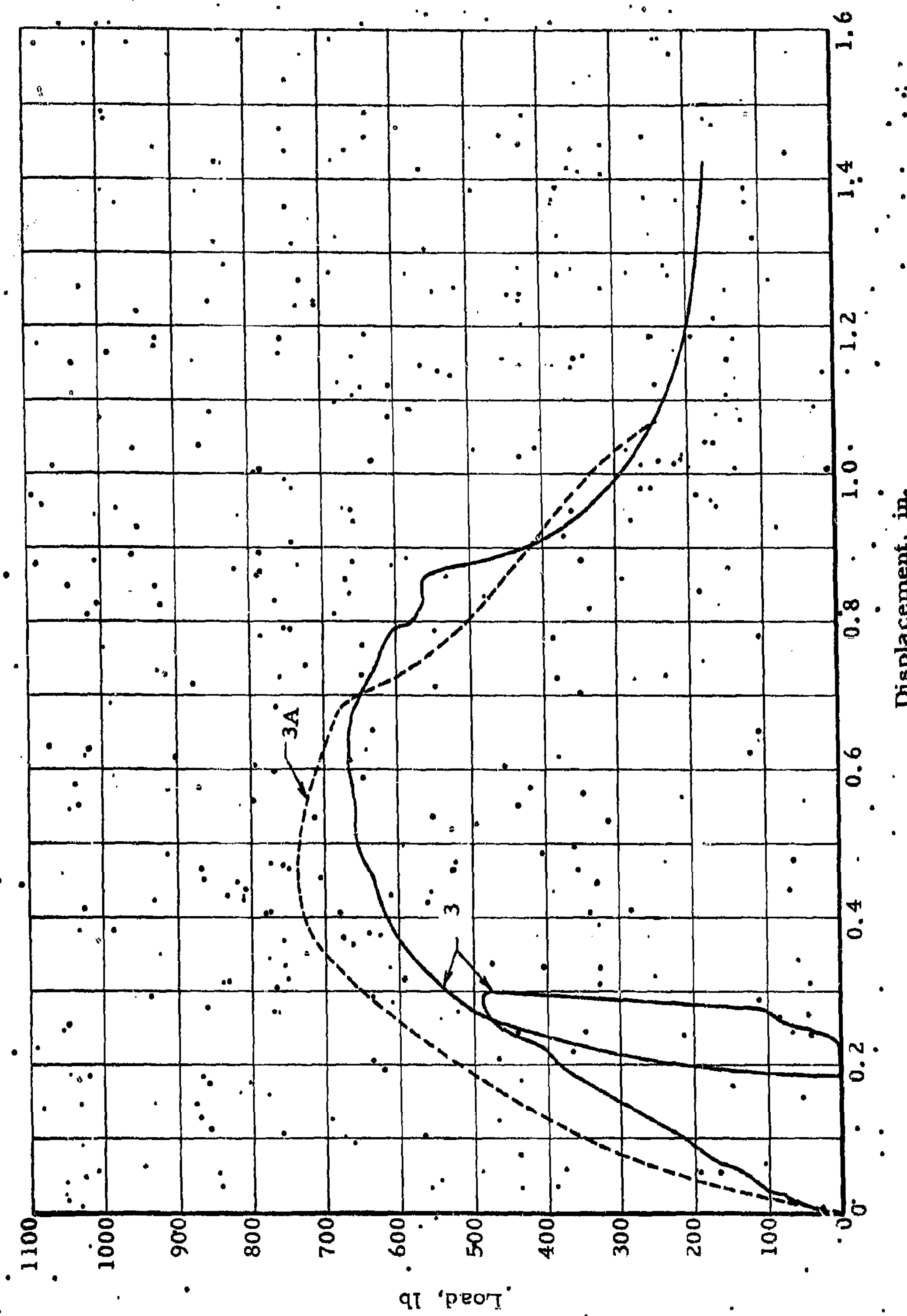

Fig. F-6 STATIC LOAD-DISPLACEMENT FOR FOOTING ON COHESIVE MATERIAL
(Exper. No. 3 and 3A)

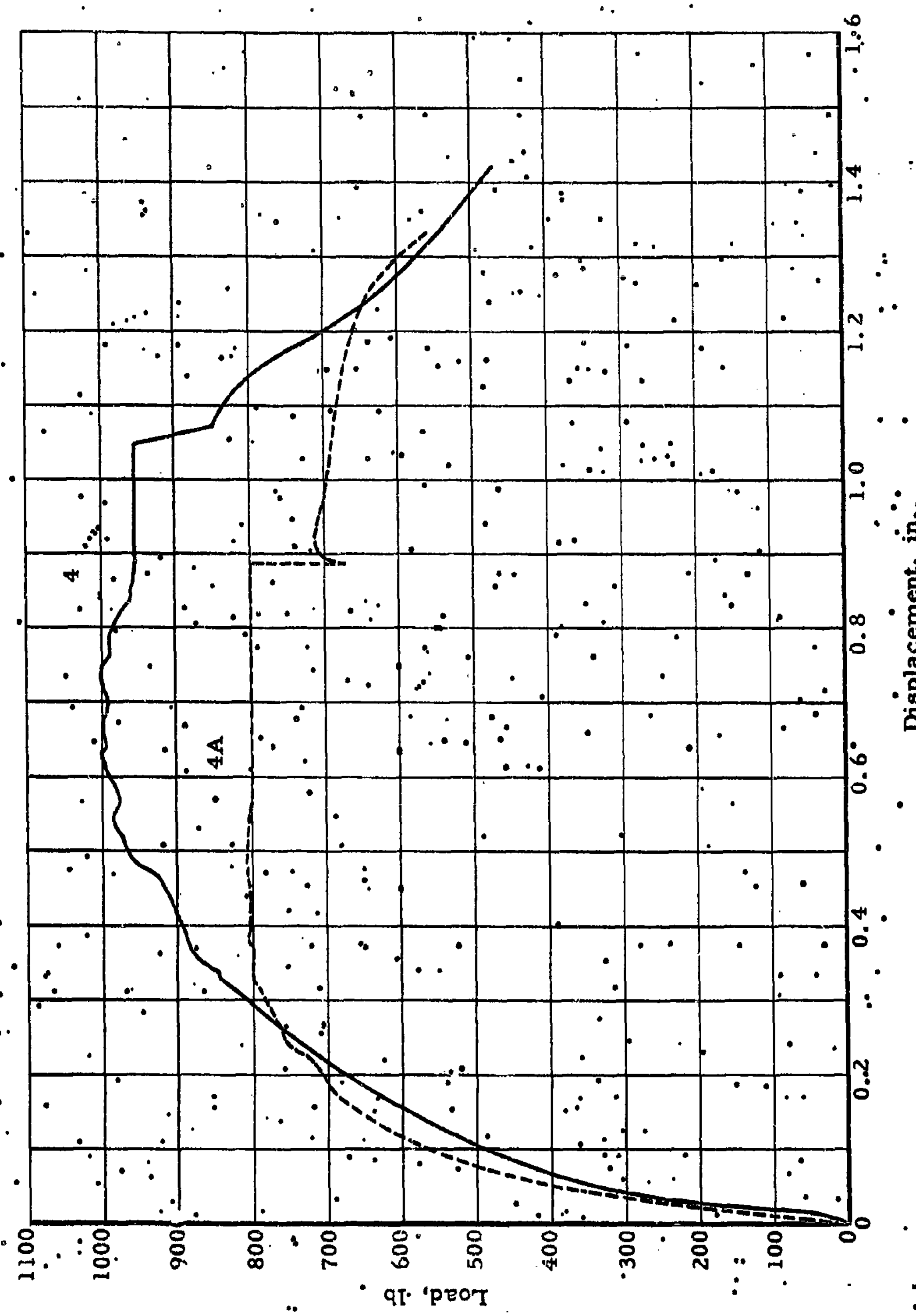

Fig. F-7 STATIC LOAD-DISPLACEMENT FOR FOOTING ON COHESIVE MATERIAL
(Exper. No. 4 and 4A)

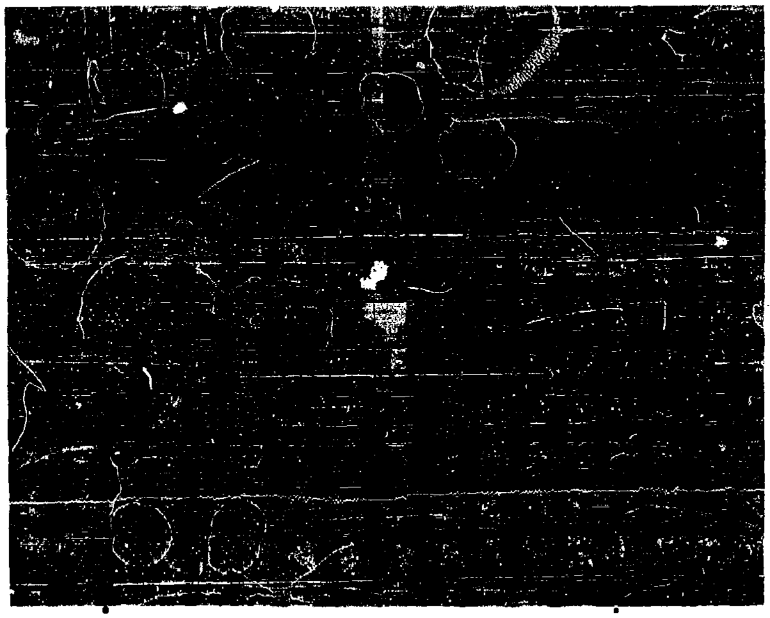

Fig. F-8 FAILURE OF 1-IN. FOOTING ON COHESIVE SOIL
(Exper. No. 7)

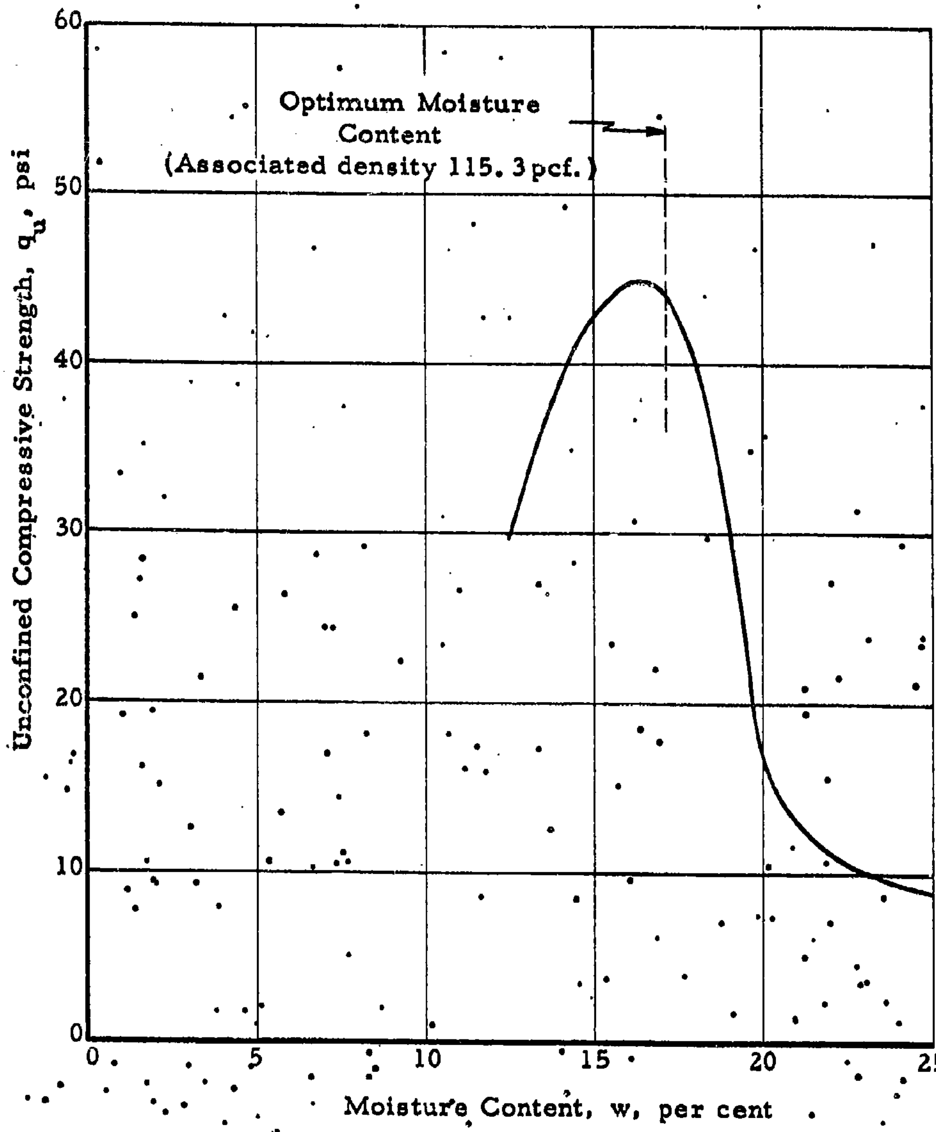

Fig. F-9 RELATIONSHIP OF UNCONFINED COMPRESSIVE STRENGTH TO MOISTURE CONTENT

APPENDIX G

NOMENCLATURE

APPENDIX G

NOMENCLATURE

A	=	area
B	=	footing width
c	=	cohesion
D	=	depth of burial
g	=	gravitational constant
I	=	inertia
M	=	moment
m	=	mass
N_c, N_q, and N_γ	=	dimensionless bearing capacity factors
P	=	force
P_s	=	static capacity
q	=	bearing capacity
$q_\square$	=	bearing capacity of square footing
q_u	=	unconfined compressive strength
R	=	resistance
r	=	distance
t	=	time
w	=	water content
γ	=	density of soil
θ	=	angle
$\ddot{\theta}$	=	$d^2 \theta/dt$ = angular acceleration
λ	=	$\tan^{-1}$ (D/r-B)
ϕ	=	angle of internal friction

APPENDIX H

R E F E R E N C E S

APPENDIX H

REFERENCES

(1) Anderson, P., SUBSTRUCTURE ANALYSIS AND DESIGN, p. 87, The Ronald Press, New York (1956).

(2) Armour Research Foundation, GROUND SHOCK ISOLATION OF BURIED STRUCTURES, Contract No. AF(601)-1134, results to be published.

(3) De Beer, E. and Wallabs, M., "Limitation of the Validity of Application of the Formulas from Prandtl-Buisman and from Anderson for the Ultimate Bearing Capacity of Soil underneath Footings" p. 63-68, Proc. 2nd. Inter. Conf. on Soil Mech. Foundation Engr. 1 (1949).

(4) Hasson, R. R. H., "An Analytical Investigation of Krey's Theory of Foundation Failure", thesis, Illinois Institute of Technology, Chicago (June 1959).

(5) Hodge, P. G. jr., "The Method of Characteristics Applied to Problems of Plane Plastic Strain with Inertial Effects", Appendix B., DESIGN AND ANALYSIS OF FOUNDATIONS FOR PROTECTIVE STRUCTURES, Interim report, AFCWC-TN-60-36 by K. E. McKee (reference 12).

(6) Landale, T. S., "Investigations into the Dynamic Bearing Properties of Cohensionless Soils", thesis, Massachusetts Institute of Technology, Cambridge (Sept. 1954).

(7) Massachusetts Institute of Technology, BEHAVIOR OF SOILS UNDER DYNAMIC LOADING 3, Final report on laboratory studies, AFSWP 118 (Aug. 1954).

(8) McKee, K. E. DESIGN AND ANALYSIS OF FOUNDATION FOR PROTECTIVE STRUCTURES, AFSWC-TR-59-56, Armour Research Foundation, Chicago (Oct. 1959).

(9) McKee, K. E., op. cit. Appendix A.

(10) McKee, K. E., op. cit. Appendix B.

(11) McKee, K. E., op. cit. Appendix C.

(12) McKee, K. E., DESIGN AND ANALYSIS OF FOUNDATION FOR PROTECTIVE STRUCTURES, AFSWC-TN-60-36, interim report, Armour Research Foundation, Chicato (Sept. 1960).

(13) McKee, K. E., op. cit. Appendix E.

(14) McKee, K. E., op. cit. Appendix G.

(15) Selig, E. T. and Rowe, R. D. ARTIFICIAL SOILS, Armour Research Foundation, Chicago, (Sept. 1960).

(16) Spencer, A. J. M., "The Dynamic Plane Deformation of an Ideal Plastic-Rigid Solid", J. Mech. Phys. Solids. 8, 262-279 (1960).

(17) Terzaghi, K., THEORETICAL SOIL MECHANICS, Chapter XIII, John Wiley and Sons, Inc., New York (1943).

(18) Terzaghi, K. and Peck, R. B., SOIL MECHANICS IN ENGINEERING PRACTICE, John Wiley and Sons, Inc., New York (1948).

DISTRIBUTION

No. of Cys	
	HEADQUARTERS USAF
1	Hq USAF (AFOCE), Wash 25, DC
1	Hq USAF (AFCEI-ES), Wash 25, DC
1	Hq USAF (AFDRT), Wash 25, DC
1	Hq USAF (AFCIN-3B), Wash 25, DC
1	USAF Dep IG for Insp (AFCDI-B-3), Norton AFB, Calif
	MAJOR AIR COMMANDS
1	AFSC (SCR), Andrews AFB, Wash 25, DC
1	AFLC (Mr. Louis A. Nees), Wright-Patterson AFB, Ohio
1	AUL, Maxwell AFB, Ala
1	Hq, Office of Aerospace Research (RRONN), Wash 25, DC
	AFSC ORGANIZATIONS
1	BSD (WDFN, Capt Fluhr), AF Unit Post Office, Los Angeles 45, Calif
2	ASD (Tech Library, marked for Director of Sys Mgt and WWAD), Wright-Patterson AFB, Ohio
2	ESD (Tech Library, marked for CRRA and CRZG), Hanscom Fld, Bedford, Mass
	AFSWC, Kirtland AFB, NMex
1	(SWNH)
35	(SWOI)
1	(SWRS)
	ARMY ACTIVITIES
1	Director, Ballistic Research Laboratories (Library), Aberdeen Proving Ground, Md
1	Commanding Officer, US Army Engineers, Research and Development Laboratories, Ft. Belvoir, Va
1	Director, US Army Waterways Experiment Station (WESRL), P.O. Box 60, Vicksburg, Miss
2	Office of the Chief, Corps of Engineers, US Army, (Protective Construction Branch), Wash 25, DC
	NAVY ACTIVITIES
1	Chief, Bureau of Yards and Docks, Department of the Navy, Wash 25, DC
1	Commanding Officer and Director; Naval Civil Engineering Laboratory, Port Hueneme, Calif

DISTRIBUTION (Cont'd)

OTHER DOD ACTIVITIES

2	Chief, Defense Atomic Support Agency (Blast and Shock Division), Wash 25, DC
1	Commander, Field Command, Defense Atomic Support Agency, (FCAG3), Sandia Base, NMex
10	ASTIA (TIPDR), Arlington Hall Sta, Arlington 12, Va

OTHER

1	American Machine and Foundry Company, (Dr. G. Neidhardt), 7501 North Natchez Avenue, Niles, Ill
1	Paul Weidlinger, Consulting Engineer, 770 Lexington Avenue, New York 21, NY
1	University of Missouri, School of Mines and Metallurgy, (Dr. Clark), Rolla, Mo
1	Purdue University, School of Civil Engineering, (Dr. G. A. Leonards), West Lafayette, Ind
1	University of Illinois, (Dr. N. M. Newmark), 207 Talbot Laboratory, Urbana, Ill
1	University of Illinois, (Dr. H. O. Ireland), 207 Talbot Laboratory, Urbana, Ill
1	Massachusetts Institute of Technology, Department of Civil and Sanitary Engineering, (Dr. Robert V. Whitman), Cambridge 39, Mass
1	St Louis University, (Dr. Carl Kisslinger), 3621 Olive Street, St Louis 8, Mo
1	Armour Research Foundation, Illinois Institute of Technology, 3422 South Dearborn Street, Chicago 15, Ill
1	University of Massachusetts, Department of Civil Engineering, (Dr. Merit P. White), Amherst, Mass
1	Official Record Copy (SWRS)